

AN ABSTRACT OF THE THESIS OF

John T. Ebner for the degree of Master of Science in

Electrical and Computer Engineering presented on April 3, 1987.

Title: The Growth of Ternary Compound Semiconductors by Molecular
Beam Epitaxy

Redacted for Privacy

Abstract approved: _____

This thesis reports on an investigation of the growth, by Molecular Beam Epitaxy, of III,III-V ternary compound semiconductors. Strained and unstrained growth was studied via the deposition of InGaAs on GaAs and InP substrates. Lattice matched InGaAs on InP was grown, and an in situ method was developed to find the oven temperatures which yield the lattice matched composition. Lattice mismatched systems were studied experimentally by growing thin layers of InGaAs between layers of GaAs. Growth was studied via Reflection High Energy Electron Diffraction. Structural properties were studied via Auger Sputter Profiling, Secondary Ion Mass Spectrometry, and Transmission Electron Microscopy. Optical properties were studied via Photoluminescence Spectroscopy.

It is shown that lattice mismatch induced strain can significantly affect the resultant structure. One effect is a preferential migration of one constituent of the alloy to the surface. This segregation modifies the morphology of the structure altering the film's optical properties.

The Growth of Ternary Compound Semiconductors
by Molecular Beam Epitaxy

by

John Ebner

A THESIS

submitted to

Oregon State University

in partial fulfillment of
the degree requirements for the
degree of
Master of Science

Completed April 3, 1987

Commencement June 1987

APPROVED:

Redacted for Privacy

Professor of Electrical and Computer Engineering in charge of major

Redacted for Privacy

Head of Department, Electrical and Computer Engineering

Redacted for Privacy

Dean of the Graduate School

Date thesis is presented April 3, 1987

Typed by researcher for John T. Ebner

ACKNOWLEDGEMENT

I would like to acknowledge the support and guidance of my advisor, Dr. John R. Arthur, useful discussion and collaboration with Dr. Kelin Kuhn of the University of Washington, and the assistance of fellow student Xi Jin. Financial support in the form of a Materials Science Fellowship, granted by the Materials Science Committee at Oregon State University, and Chevron Scholarship, granted by the Department of Electrical and Computer Engineering, is also gratefully acknowledged.

TABLE OF CONTENTS

INTRODUCTION	1
LITERATURE REVIEW	7
EXPERIMENTAL PROCEDURE	26
EXPERIMENTAL RESULTS	35
DISCUSSION	50
SUMMARY AND CONCLUSIONS	65
REFERENCES	67
APPENDIX	70

LIST OF FIGURES

	<u>Page</u>
1. Band gap versus lattice constant for various III-V ternary semiconductors.	5
2. Photograph of a typical RHEED diffraction pattern of GaAs at a temperature of 560° C.	8
3. RHEED oscillations of GaAs growing on GaAs.	10
4. Schematic of a (100) growing surface.	11
5. Schematic of an off axis (100) growing surface.	12
6. Critical thickness for misfit dislocation formation for InGaAs grown on GaAs.	18
7. Perturbation on semiconductor band structure due to biaxial strain.	20
8. Auger electron spectra of a contaminated InP surface.	30
9. Schematic of InGaAs structures grown on GaAs.	33
10. RHEED oscillations of strained InGaAs growing on GaAs.	36
11. Indium oven flux as a function of oven temperature as measured by RHEED oscillations and flux monitor.	37
12. Photographs of RHEED patterns, of InGaAs grown on InP, with arsenic and gallium stabilized surface reconstructions.	38
13. RHEED oscillations of tensionally strained, unstrained, and compressively strained InGaAs growing on InP.	40
14. SEM micrograph of surface defects on a 1 micron thick lattice matched InGaAs film grown on InP.	41
15. PI spectrum from a 1 micron thick InGaAs film lattice matched to InP.	42
16. Auger profiles of InGaAs grown on GaAs at various substrate temperatures between 495° C and 590° C.	44
17. PI spectra from 75 angstrom In _{.20} Ga _{.80} As quantum wells grown at substrate temperatures between 495° C and 590° C.	45
18. SIMS spectra of quantum wells of In _{.05} Ga _{.95} As and In _{.10} Ga _{.90} As grown on GaAs.	46

19.	TEM micrographs of $\text{In}_{.05}\text{Ga}_{.95}\text{As}$ and $\text{In}_{.10}\text{Ga}_{.90}\text{As}$ quantum wells grown on GaAs.	48
20.	PL spectra of quantum wells of $\text{In}_{.05}\text{Ga}_{.95}\text{As}$ and $\text{In}_{.10}\text{Ga}_{.90}\text{As}$ grown on GaAs.	49
21.	RHEED oscillation of InGaAs growing on GaAs.	51
22.	Auger sputter profile of 75 angstroms of $\text{In}_{.20}\text{Ga}_{.80}\text{As}$ capped by 75 angstroms of GaAs grown at a substrate temperature of 570° C at two different arsenic fluxes.	53
23.	The ratio of the initial surface concentrations of indium to gallium, on 75 angstroms of $\text{In}_{.20}\text{Ga}_{.80}\text{As}$ capped by 75 angstroms of GaAs, as a function of substrate temperature.	55
24.	Band diagram of InGaAs quantum well grown on GaAs showing the effects of segregation induced composition grading.	57
25.	RHEED oscillations from compressively strained InGaAs growing on GaAs, and on InP.	58
26.	The band gap of unstrained InGaAs, and InGaAs grown on GaAs as a function of indium mole fraction.	61
27.	Calculated and measured quantum well transition for $\text{In}_{.05}\text{Ga}_{.95}\text{As}$ and $\text{In}_{.10}\text{Ga}_{.90}\text{As}$ single quantum wells.	62
28.	Schematic of the interactions occurring on growing strained surface.	64

THE GROWTH OF TERNARY COMPOUND SEMICONDUCTORS BY MOLECULAR BEAM EPITAXY

INTRODUCTION

Research in materials science is driven by the need for new materials. Today's machines are limited by the materials which are available, and development of the next generation of machines will only be possible in conjunction with the development of the materials which allow a designer to break free from the constraints which were imposed upon his predecessors. As new material systems become available, product ideas which in the past were not feasible become so, which in turn stimulates more research. This cycle is now occurring in the area of III-V semiconductors.

III-V semiconductors are compounds composed from Group IIIa and Group Va elements. Particularly interesting are those which crystallize in the zincblende structure. Of the many properties of these materials two attributes have aroused the most commercial interest: the electron mobility and the band structure. The electron mobility is a measure of how an electron in the material reacts to an applied electric field. This is important in transistor operation, limiting the speed at which a transistor can switch. The band structure, among other things, describes how the material will interact with light, in particular the energies at which the interaction is most efficient. This is important in the operation of optical sources and detectors.

The III-V semiconductor system most studied is GaAs. The electron mobility of GaAs is six times that of silicon. This difference raises the hope that transistors faster than those achievable in silicon can be made. GaAs is also interesting for optical devices. It

has a band structure which is direct, i.e., the lowest conduction band minimum and the highest valence band maximum are coincident in momentum. This allows for efficient absorption and emission of light.

The III-V compound semiconductors are not limited to those composed of only two elements, such as GaAs. More complicated compounds can be made of three elements, ternary alloys, or four elements, quaternary alloys. Devices, for both transistor and optical applications, constructed with combinations of these III-V semiconductors are being investigated. This interest has driven research into methods of growing composite III-V materials. Crystal growth techniques, such as Molecular Beam Epitaxy (MBE) and Metal Organic Chemical Vapor Deposition (MOCVD), have been developed. These techniques allow thin crystal films to be grown on planar crystalline substrates and offer the possibility of creating both binary compound semiconductors and more complicated alloys.

The epitaxial growth method utilized in this work was MBE. In this technique elemental sources are heated in Ultra High Vacuum (UHV) to develop a desired evaporative flux. A heated crystalline substrate is then exposed to these fluxes. The impinging elements react on the substrate surface to form the film which grows using the crystal structure of the substrate as a template. The flux of the Group Va element is set higher than that of the Group IIIa element. This creates a situation in which the Group IIIa element is the rate limiting species in the growth reaction, and its flux determines the growth rate.

In the growth of a ternary material composed of two Group IIIa elements and one Group Va element, e.g., AlGaAs, the composition of the

epitaxial layer is determined by the flux ratio of the rate limiting species, the Group IIIa metals. The fluxes are determined by the oven temperatures, and the vapor pressure of the material in the crucibles. Accurate composition control in the growing film can be achieved by precise control of the temperature of the source ovens.

The composition of a growing ternary film can be changed gradually by varying the oven temperatures of the Group IIIa elements, or abruptly through the use of shutters located in front of each oven. The time it takes to open or close a shutter is short compared to the time it takes to grow one atomic layer of material. This allows the creation of interfaces between two materials which are almost perfectly abrupt. An abrupt interface between two dissimilar materials in a crystal is known as a hetero-interface. The ability to construct these materials permits investigation into both the bulk properties of ternaries and the properties of novel devices involving hetero-interfaces. These are materials and structures which are difficult, if not impossible, to produce by melt growth techniques due to immiscibility in the solid solution or abrupt changes in film composition.

The hetero-interface system most thoroughly studied consists of GaAs and AlGaAs. This is due to the close match between the lattice constant of AlGaAs and GaAs. AlGaAs has a lattice constant that varies linearly between that of AlAs, 5.661 angstroms, and that of GaAs, 5.653 angstroms, depending upon the mole fraction of aluminum in the film¹. This close matching to the lattice constant of GaAs allows easier epitaxial growth of hetero-structures comprised of this family of compounds.

Problems arise in the growth of other ternaries due to the lack of a substrate with a similar lattice constant as the film being deposited. Figure 1 shows the relationship between lattice constant and band gap for a number of III-V ternary compound semiconductors. The commonly available single crystal III-V substrate materials are GaAs and InP. The lattice constants of these are 5.633 angstroms and 5.869 angstroms, respectively³. As can be seen in Figure 1 only a few ternary systems have the same lattice constant as these two substrate materials. The majority of compound semiconductors have a different lattice constant and therefore are under strain when grown on either of these two substrate materials. The effects that this strain has on the morphology of the film as it grows, and the resultant properties of the film, are not well understood.

When a thin film having one lattice constant is grown on a substrate having another the whole structure deforms elastically. The amount of strain accommodated by each material is dependent upon its respective elastic constant and thickness. In general the substrate is so much thicker than the film that the film is either stretched or compressed such that it assumes the lattice constant of the substrate⁴. This has a number of different effects on the film, e.g., morphologic changes can occur during growth as a result of this strain. The film configures itself in its lowest energy form as it grows, but as it gets thicker the strain energy builds. After a certain thickness it becomes energetically favorable to form dislocations to relieve this strain⁴. These misfit dislocations can have catastrophic consequences on film quality.

Misfit formation is not the only morphologic result of strained

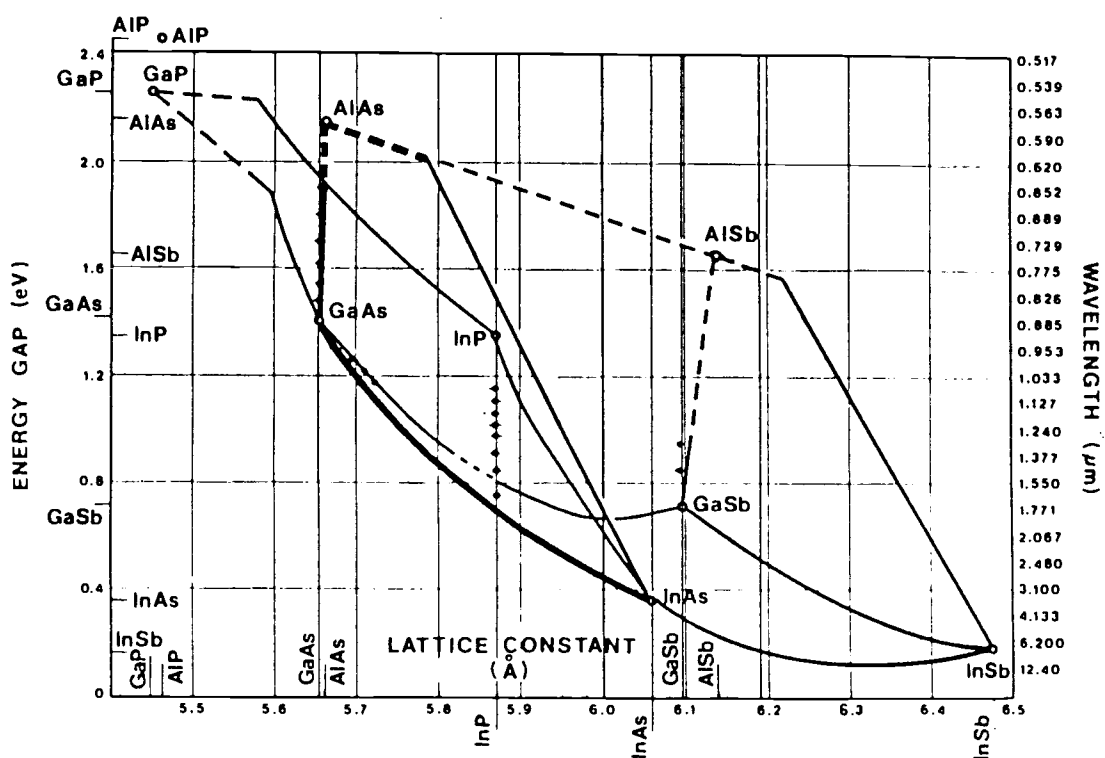


Figure 1
Band gap versus lattice constant for various III-V ternary compound semiconductors². The number of ternaries which lattice match to either GaAs or InP is small.

growth. One of the experimental observations in this work is the preferential migration, or segregation, of one constituent of a ternary alloy to the surface during growth, where it either collects or evaporates. This brings the lattice constant of the film closer to that of the substrate, thus lowering the total energy of the film. Segregation can degrade the abruptness of hetero-interfaces, and alter the composition profile of the film from what was desired⁵.

To utilize the potential of strained ternaries and heterostructures made with them the problems associated with their growth need to be studied. The growth of one ternary, InGaAs, grown on GaAs and InP substrates was investigated in this work. InGaAs has a lattice constant which varies linearly between that of GaAs, 5.653 angstroms, and that of InAs, 6.088 angstroms³. This allows the growth of InGaAs either compressively strained on GaAs, or compressively strained, tensionally strained, or unstrained on InP.

LITERATURE REVIEW

There are three areas of previous work to review in order to appreciate the problems in growing InGaAs. These areas are: MBE growth of lattice matched materials, strain induced effects, and previous work on the growth of indium compounds.

As described in the introduction, the growth of GaAs by MBE occurs when gallium and arsenic are simultaneously deposited onto a heated GaAs substrate. An understanding of the atomistic details of how these constituents interact with each other, and the substrate, is the goal of the present section.

An informative technique used to monitor the structure of a crystal surface is Reflection High Energy Electron Diffraction (RHEED). In this technique high energy electrons are focused onto the crystal surface at glancing incidence. The electrons scatter off the surface and create an interference pattern which is related to the periodicity of the atomic arrangement of the surface. This pattern is displayed on a phosphor screen which is mounted perpendicular to the surface, at the reflected angle of the electron beam. A photograph of a typical GaAs RHEED pattern is shown in Figure 2. The bright spot in the center, labeled (a) is the specular reflection. The streaks labeled (b) are integral order diffraction which is related to the bulk atomic spacing. The faint streaks labeled (c) are $1/2$ order diffraction features. These imply an additional periodicity exists on the surface which has twice the spacing as the bulk atom spacing. This is due to surface reconstruction, which arises from surface atoms shifting slightly in position in order to minimize total surface energy.

The growth of a mono-layer of material can be observed in the

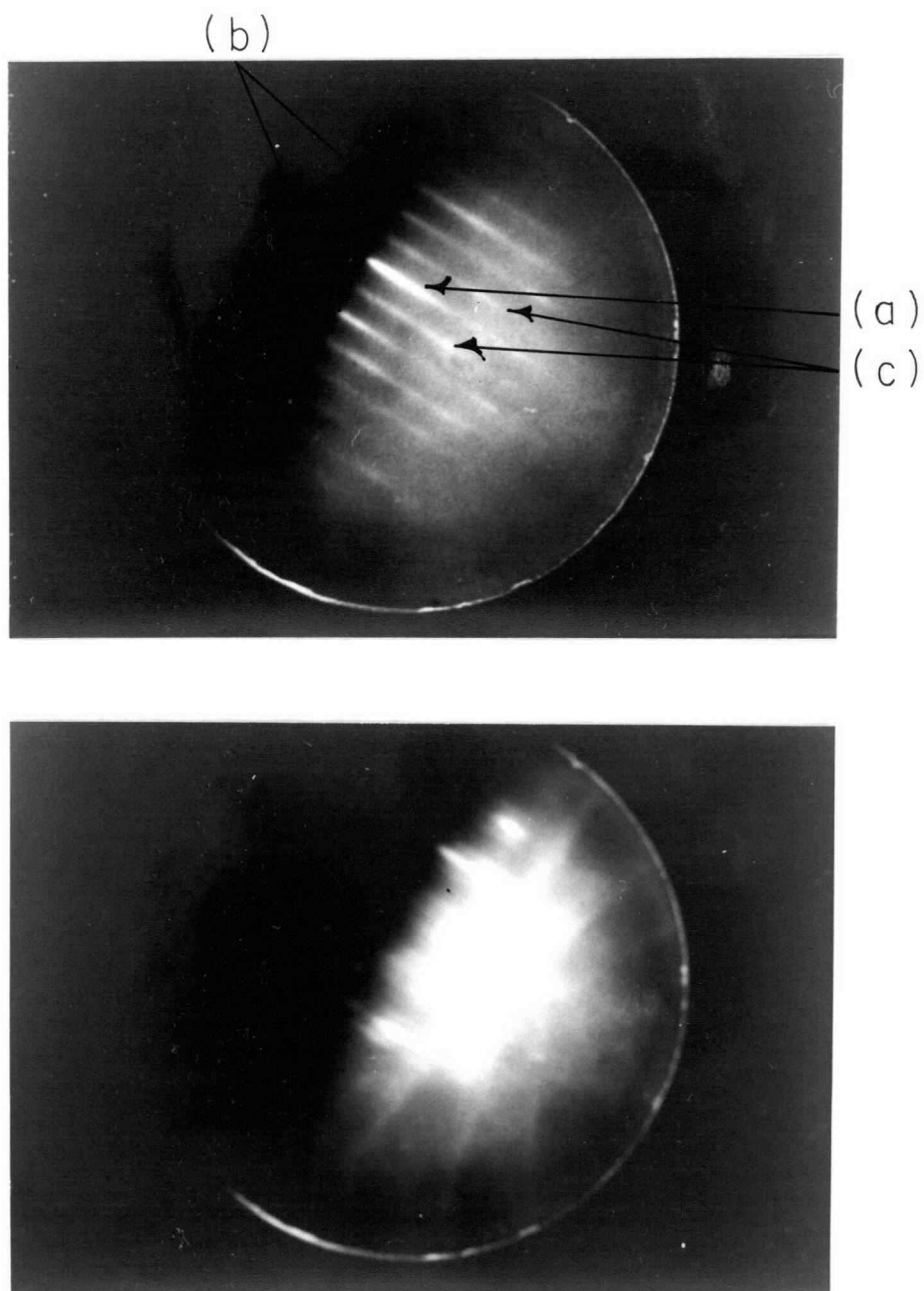


Figure 2

Photograph of a typical RHEED diffraction pattern of GaAs at a temperature of 560° C. The specular reflection is labeled (a), (b) labels the integral order diffraction features, and (c) labels diffraction due to surface reconstruction. The lower photograph is obtained by rotating the crystal 90° from the azimuth used for the upper photograph.

RHEED pattern. It is seen as an oscillation in the intensity of the RHEED features. A measurement of the specular diffraction spot as a function of time from the onset of growth is given in Figure 3. The morphology of the surface after growth and subsequent anneal is very flat. This gives rise to a high diffraction intensity, (a) in Figure 3. As gallium is introduced onto the surface, by opening the shutter in front of the gallium oven, (b), a new mono-layer is nucleated. This increases the microscopic roughness of the surface and decreases the diffraction intensity. The diffraction intensity decreases until at $1/2$ mono-layer coverage a minimum in intensity is reached, (c). As this mono-layer fills in, the diffraction intensity again increases to a maximum, (d). This process repeats as new layers form on completing previous ones⁶. A schematic of the crystal surface during this process is shown in Figure 4.

During growth there are a number of competitive processes which determine the resultant surface morphology. The competition is between growth by nucleation of new layers, and growth by addition to the edges of existing layers. In the above description it was assumed that new layers were nucleated, modulating the microscopic surface roughness. It is this process which gives rise to the RHEED intensity oscillations. This will be the dominant process if the average distance between edges on the surface is longer than the average diffusion length of a gallium atom on the surface. If the average distance between step edges is shorter than the average diffusion length of gallium on the surface, the gallium will simply add to the existing steps and no RHEED oscillations will occur⁷. These two modes of growth are shown schematically in Figure 5 (a). The step density on

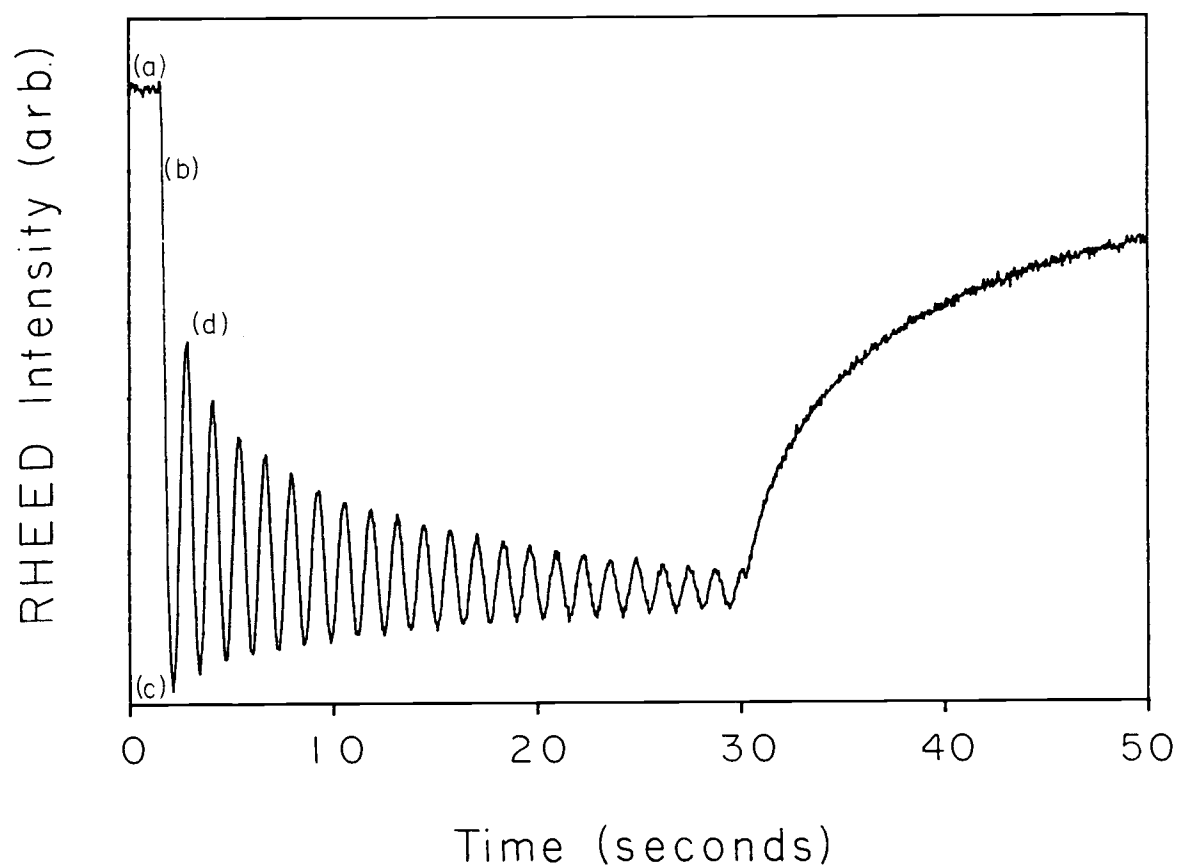


Figure 3

RHEED oscillations of GaAs growing on GaAs. The annealing surface shows bright diffraction (a), at (b) the shutter in front of the gallium oven is opened. The surface is maximally rough at (c) with $\frac{1}{2}$ mono-layer coverage, and at (d) the surface smoothes with the completion of one mono-layer.

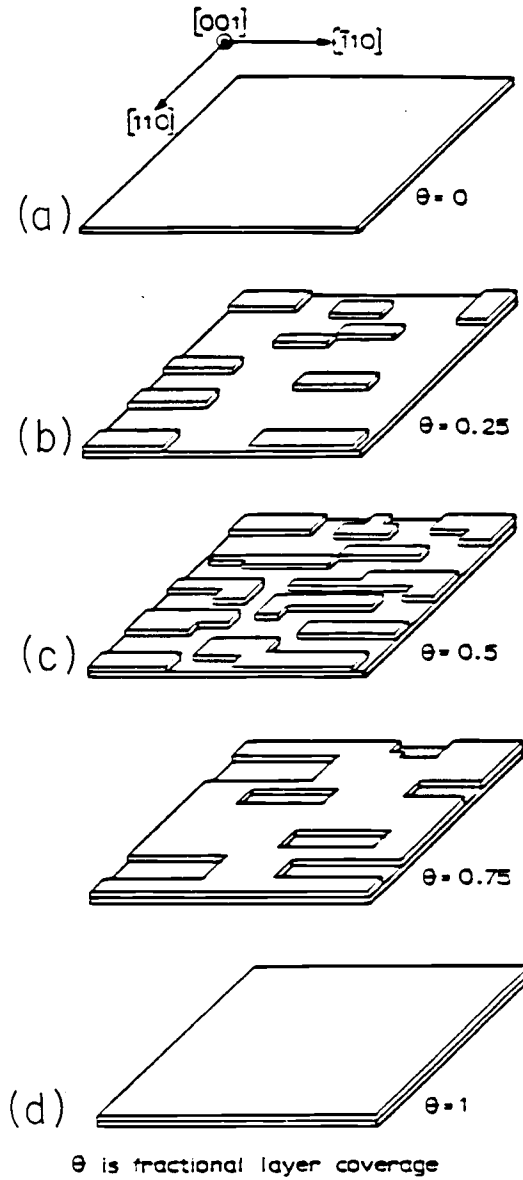


Figure 4
Schematic of a (100) growing surface⁶. The annealed surface which yields bright diffraction intensity is shown in (a). The gallium shutter is opened in (b) and the microscopic surface roughness increases as GaAs nucleates on the surface, (c) shows $1/2$ mono-layer coverage, and (d) the completion of a full mono-layer.

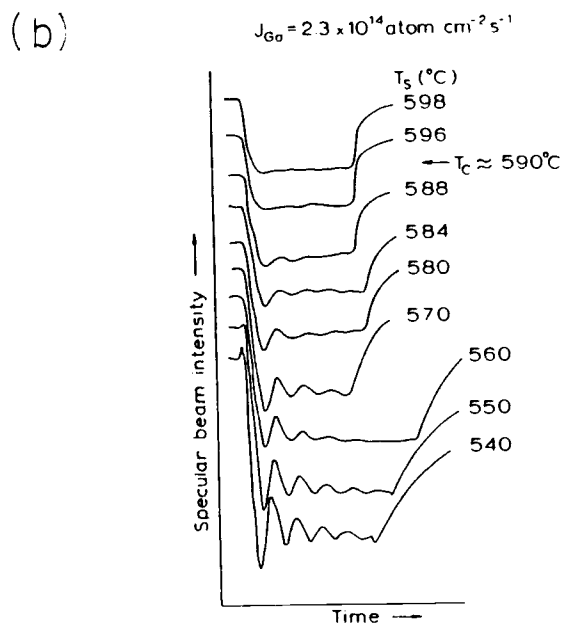
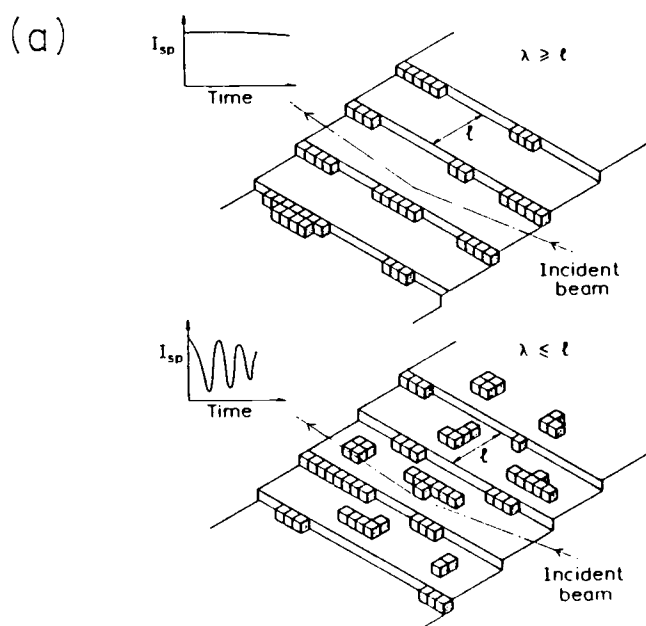


Figure 5

Schematic of an off axis (100) growing surface⁷. The two modes of growth are shown in (a), step growth in the upper diagram in which the gallium atoms find growth sites on existing step edges, and nucleated growth on the lower diagram in which gallium nucleates new steps. In (b) RHEED oscillations are shown as a function of substrate temperature. The temperature at which the transition between the two modes of growth is made is labeled T_c .

the surface is determined by the exact angle at which the crystal is cut away from the (100) orientation. When the crystal is cut close to the (100) there will be large terraces and few steps. As the orientation is tilted from the (100) the step density increases, and correspondingly the average distance between steps decreases.

These ideas concerning the interaction between the gallium migration, and the surface step density have been tested by J. H. Neave and co-workers⁷. Growing on a GaAs surface with known misorientation they studied diffraction oscillations as a function of growth rate and substrate temperature. At a given growth rate RHEED oscillations were recorded at various substrate temperatures. The diffusion length of gallium is a strong function of temperature, and at a particular substrate temperature the oscillations no longer occurred, as shown in Figure 5 (b). This was taken to be the transition temperature between the two modes of growth: step growth at higher temperatures and nucleated growth at lower temperatures. From this data taken at a number of different growth rates, and from the calculated terrace width based on the known misorientation, the surface diffusion constant for gallium was extracted⁷.

In the growth of lattice matched ternaries, such as AlGaAs on GaAs, the mechanism is complicated by the addition of a second Group IIIa element to the growing surface. AlGaAs ternaries are typically grown in the temperature range between 650° C and 680° C. At these temperatures there is appreciable decomposition of GaAs and reevaporation of gallium and arsenic. In recent work by J. M. Van Hove and P. I. Cohen RHEED oscillation measurements of both GaAs and AlGaAs were used to study this⁸. Their results indicate not only that GaAs

decomposes at these higher growth temperatures, but also that the net incorporation rate, or sticking coefficient, of gallium is a function of the aluminum mole fraction in the film being grown. The aluminum in the growing film tends to increase the incorporation of gallium. These interactions, the decomposition of GaAs, and the affect of aluminum mole fraction on gallium incorporation, make growing a film with a specific composition difficult.

A number of attempts have been made recently at extending the theoretical model concerning the microscopic interactions on a growing surface to include ternaries. One of the most illustrative of these is the work by J. Singh and co-workers⁹. In their work the growth process is modeled, via Monte Carlo computer simulation, in a manner similar to the original description of J. R. Arthur¹⁰. Gallium, evaporated from an elemental source, impinges upon the film as atoms. Arsenic sublimates from the solid and arrives at the growing surface as tetramers, As_4 . Arsenic molecules impinging on the surface incorporate through a process of dissociative chemisorption. In this process As_4 adsorbs onto the surface, and remains in this form until it either incorporates, or desorbs. The incorporation of arsenic occurs with high probability where there are two adjacent arsenic vacancies on the surface. These configurations catalyze the dissociation of the tetramer with the inclusion of the arsenic and the gallium into the growing film.

The motion of Group IIIa elements on the surface, and the process by which both the Group IIIa and Group Va species desorb, are also modeled. These processes are assumed to have standard Arrhenius form, viz., an exponential function of temperature. The activation energy of

the Group IIIa surface diffusion, or hopping, is taken to be the energy required to break the bonds which bind the element to the surface. The prefactors are inferred from experimental work in the literature.

The computations proceed by randomly depositing arsenic, gallium and aluminum onto a surface, and allowing them to move with the constraints set up by the kinetic assumptions. An interesting result which arises from the relationship between surface diffusion rate and bond strength is that certain elements are more mobile than others. The gallium- arsenic bonds are weaker than the aluminum- arsenic bonds, therefore, gallium is more mobile than aluminum on the surface at a given temperature.

This explains the need for higher temperatures in the growth of AlAs. For aluminum to have a mobility similar to that of gallium, when GaAs is grown at its optimum temperature, the substrate needs to be over 100° C hotter. In the growth of AlGaAs ternaries a smooth growing surface is difficult to obtain because the aluminum tends to nucleate new steps, instead of finding existing step edges¹¹. The substrate needs to be at a high temperature, for AlGaAs growth, to increase the mobility of aluminum and to insure a smooth surface.

This model can be scaled for the growth of other ternaries, such as InGaAs. The indium- arsenic bond is weaker than the gallium- arsenic bond. This gives rise to similar differences in surface mobility between indium and gallium, as occur between gallium and aluminum, and therefore to similar problems^{12,13}. Unfortunately, due to the dependence of lattice constant on indium mole fraction, and the resulting strain, composition control is even more important in this case.

Thus far we have only dealt with the growth of epitaxial layers in which the lattice constant difference between the film and the substrate was negligible. It is fortunate that GaAs and AlAs have such different properties, but similar structure and lattice constant. More common is the case in which the lattice constant of the film is different than that of the substrate. This situation imposes a number of constraints upon what can be grown, and the properties and morphology of what is grown.

A limit to what can be grown is embodied in the idea of critical thickness. A film with a given lattice constant and elasticity, grown on a substrate of different lattice constant and elasticity, can only be grown to a specific thickness before the strain inherent in the film causes structural changes. Most common is the formation of misfit dislocations at the interface which destroy the continuity between the film and the substrate. If the critical thickness is grossly exceeded these dislocations can bunch together and nucleate slip lines or cracks¹⁴.

A number of analyses have been performed to calculate this maximum thickness. The original calculation of J. H. Van der Merve equated the strain energy density in the film to the energy density associated with a dislocation⁴. At a certain thickness the strain energy density exceeds that of a dislocation; this is taken to be the critical thickness.

In the early 1970s J. W. Matthews and A. E. Blakeslee performed the seminal experimental work on strained overlayers, and developed another method for calculating the critical thickness¹⁵. In this work alternating layers of GaAsP and GaAs were grown on a GaAs substrate, by

Vapor Phase Epitaxy (VPE), forming a Strained Layer Superlattice (SLS). A number of these structures with different layer thicknesses and compositions were grown, and analyzed with Transmission Electron Microscopy (TEM).

A number of different dislocation structures were observed. One particular type of dislocation threaded from the substrate through the SLS. These dislocations tended to glide as they approached an interface, due to the strain in the alternate layers. If the layer was thin the dislocation continued to thread through the SLS without gliding along the interface. If the layer was thick the force on the dislocation, exerted by the strain, caused the dislocation to glide along the interface. The section of a dislocation which lay along the interface was called a misfit dislocation. The thickness at which the force on the dislocation, associated with the strain, balanced the tension in the dislocation was considered the critical thickness of the strained film¹⁵.

Recent work by R. People and J. C. Bean returns to the energy density explanation for the formation of misfits and the calculation of critical thickness¹⁶. Working in the GeSi system grown on silicon substrates, films of known composition were grown at varying thicknesses, and the misfit density measured. The possibility of these dislocations arising from the substrate is eliminated by the fact that silicon substrates are virtually dislocation free. The critical thicknesses measured were fit to a theory similar to that of Van der Merve. Figure 6 shows the critical thickness of InGaAs grown on GaAs calculated via both methods.

Misfit dislocations can alter film properties. For instance,

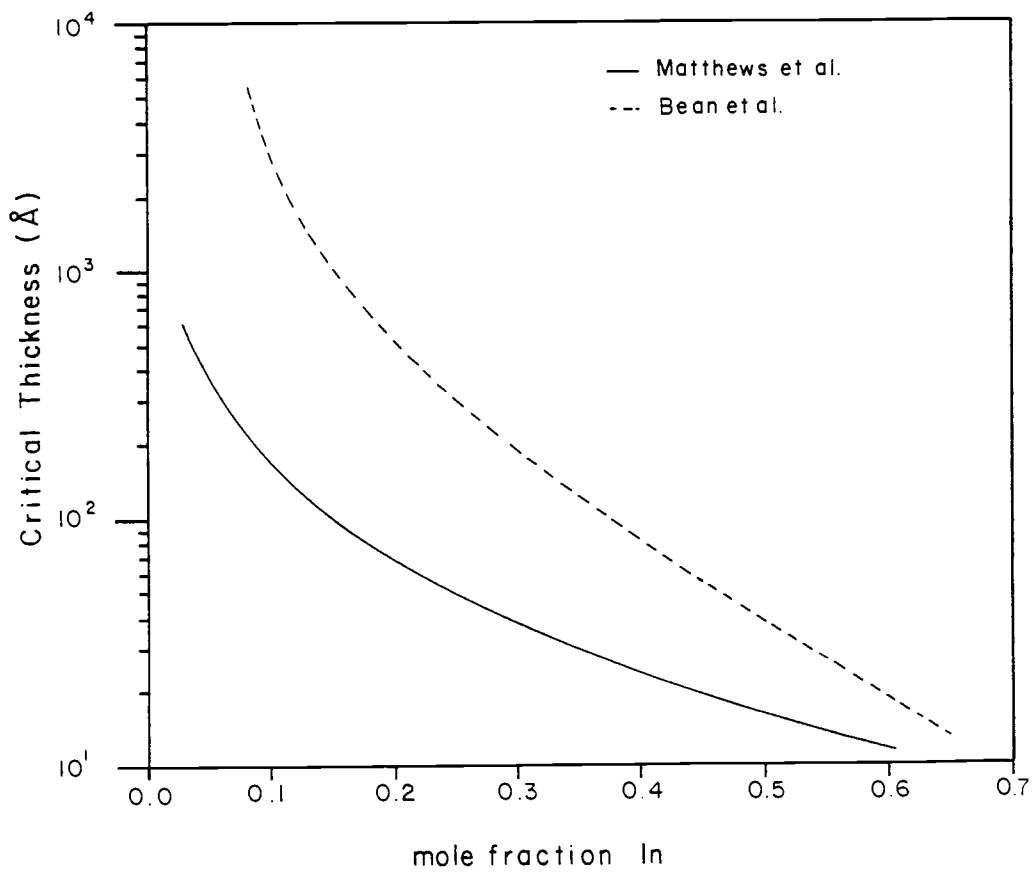


Figure 6

Critical thickness for misfit dislocation formation for InGaAs grown on GaAs. The dashed curve was derived from People's energy density theory, the solid curve was derived from Matthews's mechanical balance theory.

misfits can dramatically reduce the luminescent efficiency of an optical device. This occurs through enhanced non-radiative recombination velocity at the misfit which can destroy optical devices such as LASERs.

Even if the film is grown misfit dislocation free strain can perturb other film properties, electronic and structural. One example of how the electronic properties of a film can be altered is shown in the work of N. G Anderson and co-workers¹⁷. SLS structures consisting of alternating layers of GaAs and InGaAs were grown on GaAs substrates and Photoluminescence (PL) spectra taken. These spectra were explained using a Kronig- Penney model to calculate the optical transition energies. Strain induced perturbations on the band structure of the layers in the SLS were shown to be important in explaining the experimental data. The biaxial compressive strain in the InGaAs layers splits the valence band degeneracy and causes the bandgap to widen. A schematic of the effect of biaxial strain on band structure is shown in Figure 7.

Strain induced perturbations to the band properties increase the amount of calculation necessary in the design of a strained device. If a LASER is desired to operate at a particular energy the band structure of the unstrained ternary would have to be known, and the perturbation due to strain then included. Characterization of the unstrained ternaries is far from complete, without including the possible affects of strain.

Other structural problems can also arise in the film due to strain. One of these involves the separation of a ternary solution, which normally would be marginally stable, into its binary

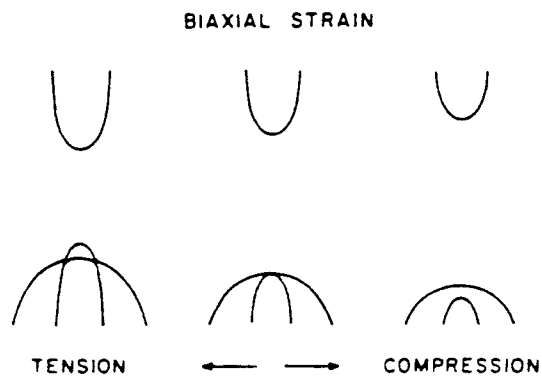


Figure 7

Perturbation of band structure due to biaxial strain¹⁷. Biaxial compressive strain widens the band gap and splits the valence band degeneracy such that the heavy hole band is above the light hole band. Biaxial tensional strain narrows the band gap and splits the valence band degeneracy such that the light hole band is above the heavy hole band. InGaAs can be grown on InP with either strain, and when grown on GaAs is under compressive strain.

constituents¹⁸. There is evidence that this could be a problem in the InGaAs system at MBE growth temperatures when the composition is close to that which lattice matches to InP¹⁹, although no experimental observations of strain induced immiscibility have yet been made.

An important effect of strain which is known to occur during MBE growth involves segregation. Dopants expected to be uniformly distributed in the film, migrate to the surface. One system in which this occurs is that of tin doped GaAs grown by MBE^{20,21}. Tin, being lower than gallium in the periodic table, has a larger tetrahedral radius. It thus develops strain when grown in GaAs on a GaAs substrate.

This has been observed experimentally by a number of research groups, but explained best by A. Rockett and co-workers²¹. In their work, what should have been a uniformly tin doped GaAs film was grown. Secondary Ion Mass Spectrometry (SIMS) was performed on the resultant structure to measure the tin composition profile. It was found that there was an excess of tin at the surface, the concentration leveled out in the majority of the film, and depleted at the film substrate interface.

The mechanism which created this doping profile was modeled with two competing processes: segregation of tin to the surface, and diffusion of tin back into the growing film. The segregation is driven by the fact that tin substitutes for gallium in GaAs, but it is larger than gallium and is therefore under strain. This strain acts as a driving force in moving tin to the surface where it is accommodated with lower energy²². This creates a flux of tin to the surface as the film grows.

The segregation flux is ultimately balanced by a diffusion flux. At the onset of growth there is no tin on the surface. As the film grows tin segregates increasing the surface concentration. As the concentration builds so does the concentration gradient between the surface and the bulk. This gradient creates a diffusion flux which drives tin back into the film. The magnitude of this flux increases as the gradient increases, and correspondingly so does the amount incorporated. These processes ultimately achieve a balance, which yields a constant tin concentration in the majority of the film. When growth is terminated the amount of tin on the surface is orders of magnitude larger than the steady state bulk concentration²¹.

There are a number of similarities, and differences, between the growth of tin doped GaAs on GaAs, and the growth of InGaAs on GaAs. Tin and indium are in the same row in the periodic table, and thus have similar tetrahedral radii. They would thus develop similar strain when incorporated in GaAs. An important difference is the amount of oversized species in the film. In the case of tin doping a number of concepts from dilute solution theory²² were easily incorporated into the model, while between 5 and 20 percent indium, in InGaAs, it is far from a dilute solution. Independent of these differences the similarities between these two systems were strong enough to act as motivation to look for similar effects.

A number of research groups have been investigating InGaAs grown by MBE. The majority have been studying devices rather than growth though. A number of different devices have been constructed in InGaAs, grown on both GaAs, and InP. These include LASERS^{23,24}, optical detectors²⁵, and High Electron Mobility Transistors (HEMT)²⁶.

Studies of the growth of these materials fall into two categories: growth on InP and growth on GaAs. The constraints imposed by growth on InP substrates involve achieving the proper fluxes of Group IIIa metals such that the resulting film has a lattice constant which matches that of InP to within .1 percent²⁷. The lattice matched composition is $\text{In}_{.47}\text{Ga}_{.53}\text{As}$. The high precision with which this needs to be set is determined by misfit dislocation formation.

There is little in the literature on how to achieve this ratio. Typically the initial calibration is done using a Quadrupole Mass Spectrometer (QMS) to set the flux ratios. The resultant film is then removed from the system and the film's lattice constant measured via X-Ray diffraction²⁸. This information is used to recalibrate the QMS, and another film is grown. The process is iterated until the desired accuracy in film composition is obtained.

A method of measuring the actual flux of each species, in situ, is desirable to find the lattice matched composition, and adjust for system drift. This type of procedure has been developed in this work using RHEED oscillations to measure absolute fluxes.

The constraints imposed by growth of InGaAs on GaAs have been described in the preceding section. The number of experimental verifications to these constraints are still few though. W. D. Laidig and co-workers²⁹ did structural analysis on InGaAs/ GaAs SLS layers using X-Ray diffraction and Scanning Electron Microscopy (SEM). These studies confirmed the ability to grow high quality epitaxial films virtually free of misfit dislocations when the indium mole fraction is kept low. Anomalies in the resultant structures were detected at high indium mole fraction, but none which they attributed to interactions

occurring on the growing surface.

The majority of studies involving the InGaAs system grown on GaAs, apart from those concerning devices, are PL^{30,31} and infra-red absorption studies³² of SLS and quantum well structures. A quantum well is a structure built out of hetero-interfaces in which a thin layer of narrow band gap material is grown between layers of wider band gap material. If the width of the narrow band gap material is on the order of the DeBroglie wavelength of an electron the proximity of the wider band gap materials perturbs the band properties of the structure. The new band properties can be calculated, via quantum mechanics, by solving the one dimensional finite well problem. The wider band gap material forms the barriers and the narrow band gap material forms the well. The resultant band gap of the structure can be altered by varying the thickness of the narrow band gap material, or the band gap of the barrier material. High quality quantum wells in both the InGaAs/ InP system³³ and the InGaAs/ GaAs system³⁴ have been constructed.

A study explicitly concerned with the growth of InGaAs was done by B. F. Lewis and co-workers³⁵. In this work RHEED oscillations of InGaAs grown on GaAs were measured. A number of novel features in the RHEED oscillations were observed and related to roughening of the surface as the InGaAs was grown. The fundamental observation in this work was that the RHEED pattern became spotty after deposition of a small number of mono-layers of InGaAs. This spotty or transmission pattern was hypothesized to arise from three dimensional growth on the surface scattering the electron beam. This type of growth is undesirable as it usually yields lower film quality, and alternative

growth procedures were attempted to circumvent this. This work has lead to a number of achievements, e.g., high quality GaAs/ InAs SLS structures on GaAs have been grown³⁶.

The work published by this group has raised a number of questions involving the interactions occuring on the surface during strained film growth, e.g., why the growth is three dimensional. These observations, and those made in this thesis concerning segregation, show that the interactions on the growing surface are far from simple. They are none the less important to understand if robust devices are to be reproducibly made in these material systems.

EXPERIMENTAL PROCEDURE

The experimental work done for this thesis can be divided into two areas: growth of InGaAs on InP, and growth of InGaAs on GaAs. In the former the intent was to develop an in situ calibration procedure for the absolute fluxes of the Group IIIa metals indium and gallium. This would allow the oven temperatures, which yield a film with a lattice constant matched to InP, to be easily found. In the latter, strain induced effects on the growth of thin films were investigated. A Perkin Elmer 425B MBE system equipped with Scanning Auger Microscope (SAM), RHEED, and QMS, was used to grow the films.

SAM is a tool used to analyze surface chemistry. In this technique a beam of high energy electrons is focused onto the surface of interest. Low energy electrons, emitted from the excited volume by the Auger process, are collected, dispersed in energy by a Cylindrical Mirror Analyzer (CMA), and detected by an electron multiplier. Surface sensitivity comes from the limited escape depth of these low energy electrons. The Auger electron energy is related to core levels of individual atoms in the surface being studied. This allows, through the use of appropriate standards, identification of the elemental composition of the surface. The Auger microscope is located in the analysis chamber of the MBE system and can only be used to look at a surface before or after growth.

RHEED is a diffraction technique in which high energy electrons are focused onto a surface at glancing incidence. The resulting diffraction pattern is used to determine whether growth is proceeding properly. RHEED is located in the growth chamber of the MBE system, and diffraction can be done as the crystal is growing. The growth rate

of the film can be extracted from temporal measurements of the diffraction pattern. These measurements are absolute measurements of the flux of the rate limiting species and are useful in setting the oven temperatures to get a desired film composition.

The apparatus constructed to measure RHEED oscillations consists of an optic fiber which can be positioned over the diffraction feature of interest, a photomultiplier tube (PMT) as a detector, and a digital storage oscilloscope. The oscilloscope memory can be read by a computer and the data subsequently graphed on a pen plotter.

The QMS is a tool which measures the partial pressures of the system residual gases. It is constructed of an ionizer which creates ions out of residual gas molecules, a mass selector which disperses the ions in terms of their mass to ionic charge ratio, and an electron multiplier which converts the flux of ions, passing through the mass selector, to an electronic current. The QMS is used to set the Group IIIa metal, and arsenic fluxes to their approximate desired values. Absolute partial pressure measurement is difficult due to nonlinearities in the QMS as a function of ion mass, and temporal drift.

A number of other techniques were utilized to examine the properties of the final film, i.e., PL, optical microscopy, SEM, SIMS, and TEM. Optical microscopy, and SEM were used to look at surface morphology, and defect structures. PL is a technique which measures certain optical properties of the film, e.g., bandgap. SIMS and TEM were performed elsewhere with assistance by Boeing Electronic Company. These measurements yield information about the composition of the final structure.

In PL a LASER is used to generate excess electrons and holes in

the material of interest. These excess carriers recombine with one another through a variety of processes: Shockley-Read-Hall, Auger and radiative. The radiative process involves the creation of a photon. These photons are collected from the sample, dispersed in wavelength via a monochromator, and detected by either a PMT or PiN diode.

In the PL system at OSU a Spectra-Physics argon ion LASER, which generates a maximum power of 17 mW at 5145 angstroms, is used as the excitation. The luminescence is dispersed in wavelength by a Jarrell-Ash .5 meter monochromator. An S-1 photocathode PMT is used as a detector for wavelengths out to 1.0 micron, and a Ge PiN diode for wavelengths from 1.0 micron to 1.6 microns.

The information obtained via this technique is the energy of the optical transitions and their intensity relative to other, similar materials which are thought to have high luminescent efficiency. No analysis of the fine structure of the spectra was attempted as the measurement temperatures involved, 77° K and 13° K, were not low enough to obtain adequate resolution.

Proper preparation of the surface prior to growth is critical to achieving high quality films. Two steps are important in the preparation of these surfaces: polishing, and pre-growth cleaning. A procedure developed for hand polishing these materials is given in Appendix 1. It is difficult, though, to obtain a higher quality polish than that found on commercially prepared wafers.

Pre-growth cleaning consisted of a number of wet chemical treatments. A sequence of solvents, trichloroethane (TCA), acetone, methanol and de-ionized (DI) water were used to de-grease the surface. Substrates were left in each solution for 2 minutes in an ultrasonic

cleaner. Next, the wafer was etched in an attempt to remove residual polishing damage. The solution used for this was Summa Develop, sold by the Mallinckrodt Chemical Company. This solution is 5 percent choline, a strong organic base, diluted with water. The wafers were etched for 2 hours at room temperature. The etch was stopped by diluting the solution for 10 minutes in running DI water.

Other systems which were tried for this free etch were H_2SO_4 : H_2O_2 : H_2O with relative ratios of 4: 1: 1, and .3 percent bromine in methanol. There was some indication that the H_2SO_4 system removed a large portion of the damage left by the polish, but often left large pits in the surface. Bromine based free etches left a hazy surface. Summa Develop consistently left flat, carbon free, surfaces on both GaAs and InP so it was used exclusively in this work.

Subsequent to the free etch the samples were affixed onto molybdenum blocks with indium solder. They were then introduced into the MBE system and degassed on the analysis stage for a minimum of 1 hour at 350° C. Auger spectra were taken of the surface to determine whether the sample had been properly cleaned. Residues, e.g., carbon, on the initial surface have been related to the defect density on the surface of the final film. In Figure 8 an Auger spectrum of a "clean" InP surface (a) and a "dirty" one (b) are shown. The peak at 271 eV in the dirty spectrum is carbon residue. If the Auger spectrum of a particular sample showed too much contamination it was removed from the system without any growth.

The major problem in growing InGaAs on InP was finding the indium and gallium oven temperatures which yield fluxes that produce a film with the lattice matched composition. The most accurate way to

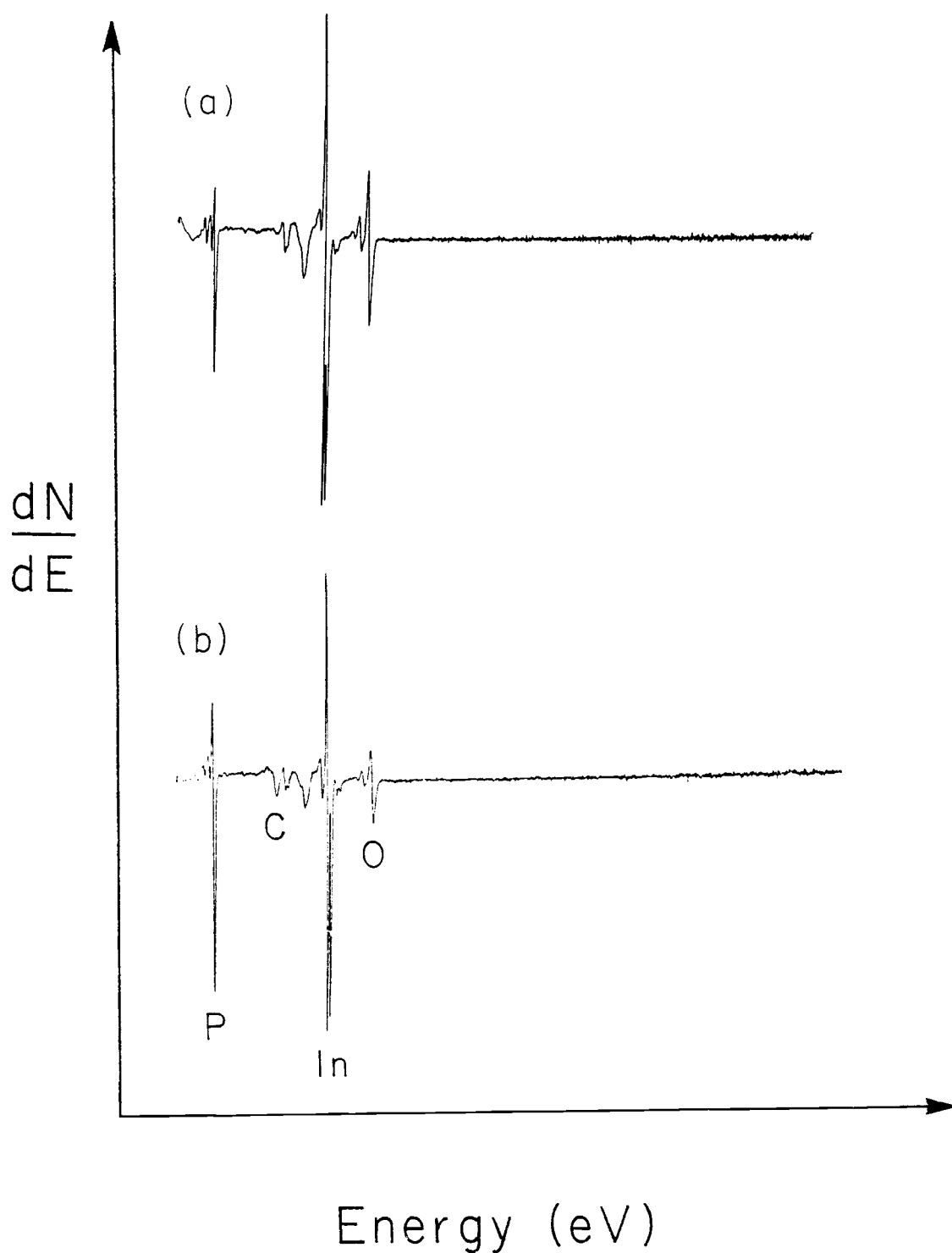


Figure 8

Auger electron spectra of InP surfaces. The upper spectra shows a clean InP surface containing only phosphorous, indium, and oxygen. The lower spectra shows a contaminated InP surface which also contains carbon.

determine these oven temperatures was by measurement of RHEED oscillations. The procedure for finding the lattice matched composition via RHEED involved measuring oscillations for the growth of GaAs on a GaAs substrate, and using the results to set the gallium oven temperature so that an absolute gallium flux of .47 mono-layers per second was obtained. Setting the indium oven temperature was more difficult. This could not be done in the same manner as was the gallium oven temperature because an InAs substrate was not available.

The flux from the indium oven was calibrated by measuring RHEED oscillations of InGaAs growing on GaAs. This could only be done at low indium mole fractions, since the RHEED pattern quickly became dim, and therefore unusable, when films with indium mole fractions above .20 were grown. Extrapolation of this flux data to higher oven temperatures yielded the setting for the desired flux of .53 mono-layers per second. The oven temperature calculated via extrapolation, which yielded the lattice matched composition, is only good to within 10° C.

The indium oven temperature was fine tuned by measuring RHEED oscillations of InGaAs growing on InP. These measurements could only be obtained when the surface reconstructed in the arsenic stabilized configuration at a substrate temperature below 500° C. At higher temperatures the metal stabilized pattern occurs and cannot be converted to the arsenic stabilized without the use of extremely high arsenic fluxes.

When the proper indium oven temperature had been found, by calibrating the growth rate of InGaAs to 1.0 mono-layer per second, growth was started. The test structure grown in all the runs was a

1.0 micron thick undoped film.

After growth the sample was removed from the system. The standard procedure for removing the indium solder, etching in concentrated hydrochloric acid (HCl), was not used (the HCl attacked the InP substrate) and indium was left on the backside. The surfaces were observed using the optical microscope, and SEM. PL was taken at 77° K using the Ge PiN diode as the detector.

A number of different investigations into strained InGaAs growth on GaAs were done. Thin, 75 angstrom, layers of $\text{In}_{.20}\text{Ga}_{.80}\text{As}$, capped with 75 angstroms of GaAs, were grown at various substrate temperatures and arsenic fluxes. A diagram of this structure is shown in Figure 9 (a). The indium composition profile was then measured via Auger sputter profiling. Similar structures consisting of 75 angstroms of $\text{In}_{.20}\text{Ga}_{.80}\text{As}$ capped with 1200 angstroms of GaAs, as shown in Figure 9 (b), were grown in the same range of substrate temperatures and PL spectra taken.

Another series of samples were grown for TEM, SIMS, and PL measurement. These consisted of a series of quantum wells, 200, 100, 50, and 25 angstroms wide, each separated by 1200 angstroms of GaAs. This structure is shown in Figure 9 (c), and allowed four quantum wells to be grown under identical growth conditions, with only the well width changing. Two InGaAs compositions, $\text{In}_{.05}\text{Ga}_{.95}\text{As}$ and $\text{In}_{.10}\text{Ga}_{.90}\text{As}$ were studied with these structures.

Oven temperature calibration via RHEED was done in all the growth of InGaAs on GaAs. To calibrate the oven temperatures for these compositions the gallium oven temperature was set to yield a flux of 1.0 minus the desired indium composition, e.g., .95 mono-layers per

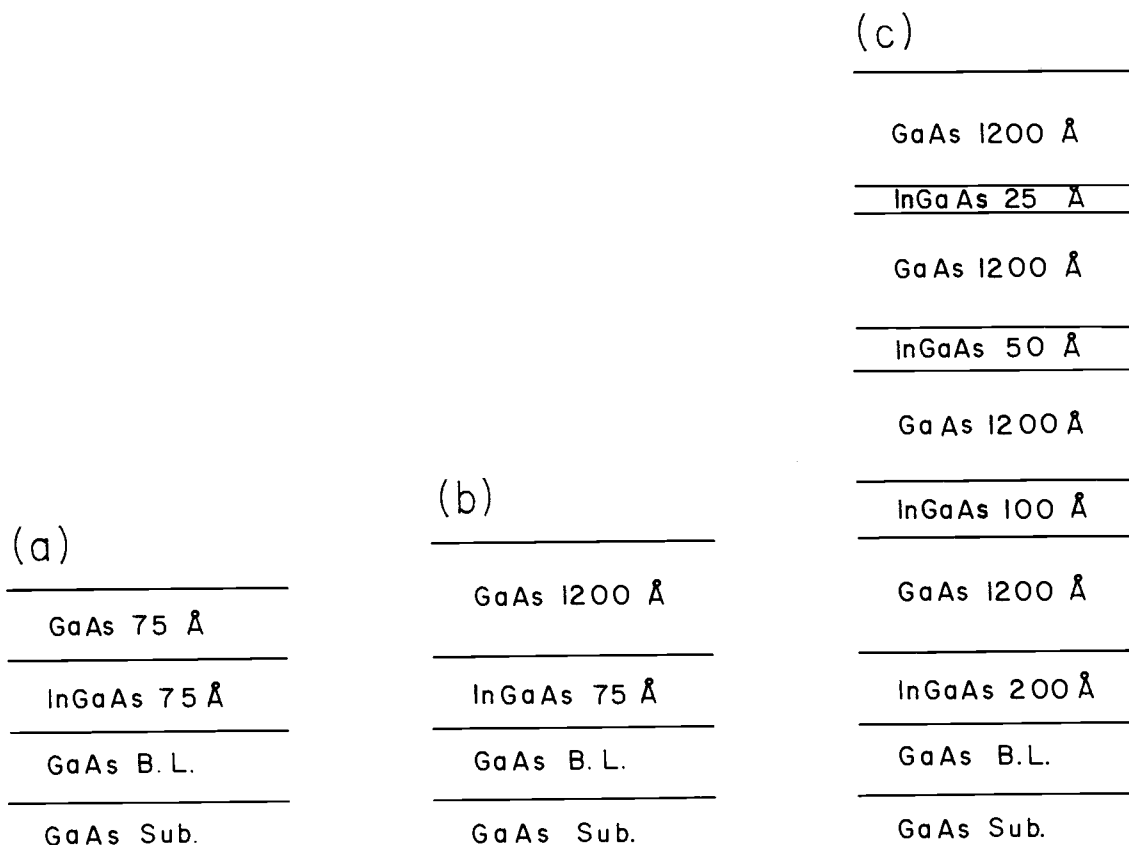


Figure 9

Schematic of InGaAs structures grown on GaAs. The structure grown for Auger sputter profiling is shown in (a), (b) shows a similar single quantum well structure grown for PI measurements, and (c) shows multiple single quantum well structures grown to investigate band gap as a function of indium mole fraction.

second in the case of $\text{In}_{.05}\text{Ga}_{.95}\text{As}$. The indium oven temperature was then set to yield a flux of indium which brought the net growth rate to 1.0 mono-layer per second. This was done on a different substrate than the one used in the experiment so that interpretation of the data was not confused.

In the Auger sputter profiling experiments the test structures were grown at various substrate temperatures. Immediately after growth the power to the substrate heater was turned off and the sample cooled. The temperature took less than 5 minutes to come down to 200°C at which point the sample was removed from the growth chamber and placed on the analysis stage. Sputtering was done with argon ions at 2 KeV, and 2.0 mA emission current. The ion pump in the analysis chamber was shut off, and an argon pressure of 3.5×10^{-5} Torr was maintained by leaking argon into the analysis chamber through a leak valve, while pumping by slightly opening the gate valve to the growth chamber. During sputtering the Auger microscope was continuously set on the 401 eV indium peak and the output was recorded on a strip chart recorder.

After profiling, the sample was placed back into the growth chamber and 2000 angstroms of GaAs were grown. The procedure was then repeated at a different substrate temperature. The substrate temperatures investigated ranged from 495°C to 590°C .

EXPERIMENTAL RESULTS

The growth of InGaAs on InP yielded a number of results: surface reconstruction as a function of substrate temperature and arsenic overpressure, RHEED oscillation measurements of strained and unstrained growth, observation of surface defects, and PL spectra.

RHEED oscillation measurements of the growth of InGaAs on GaAs were used to calibrate the indium flux. The oscillations damped quickly, as shown in Figure 10, so this could only be done at low indium concentrations. The absolute flux measured via this method, and the flux measured via the flux monitor ion gauge, are plotted in Figure 11. The indium flux, as measured by the flux monitor, can be calibrated via the oscillation measurements and the approximate indium oven temperature for growing the lattice matched composition extracted.

As noted previously RHEED oscillations of InGaAs growing on InP could only be obtained when the surface was in the arsenic stabilized reconstruction. This occurs when the substrate temperature is below 500° C, and the arsenic flux is set reasonably for growth, i.e., 3 times the gallium and indium flux. Photographs of these reconstructions are shown in Figure 12. The top pictures show RHEED diffraction from the arsenic stabilized reconstruction as viewed from the different $\langle 110 \rangle$ directions. The left picture is obtained by rotating the sample 90° from the azimuth used for the right picture. The bottom pictures show RHEED diffraction from the metal stabilized reconstructions at the same azimuths. The metal stabilized reconstructions are obtained by momentarily closing the arsenic shutter while InGaAs is growing. The reconstruction changes to metal stabilized and does not revert back to arsenic stabilized until the

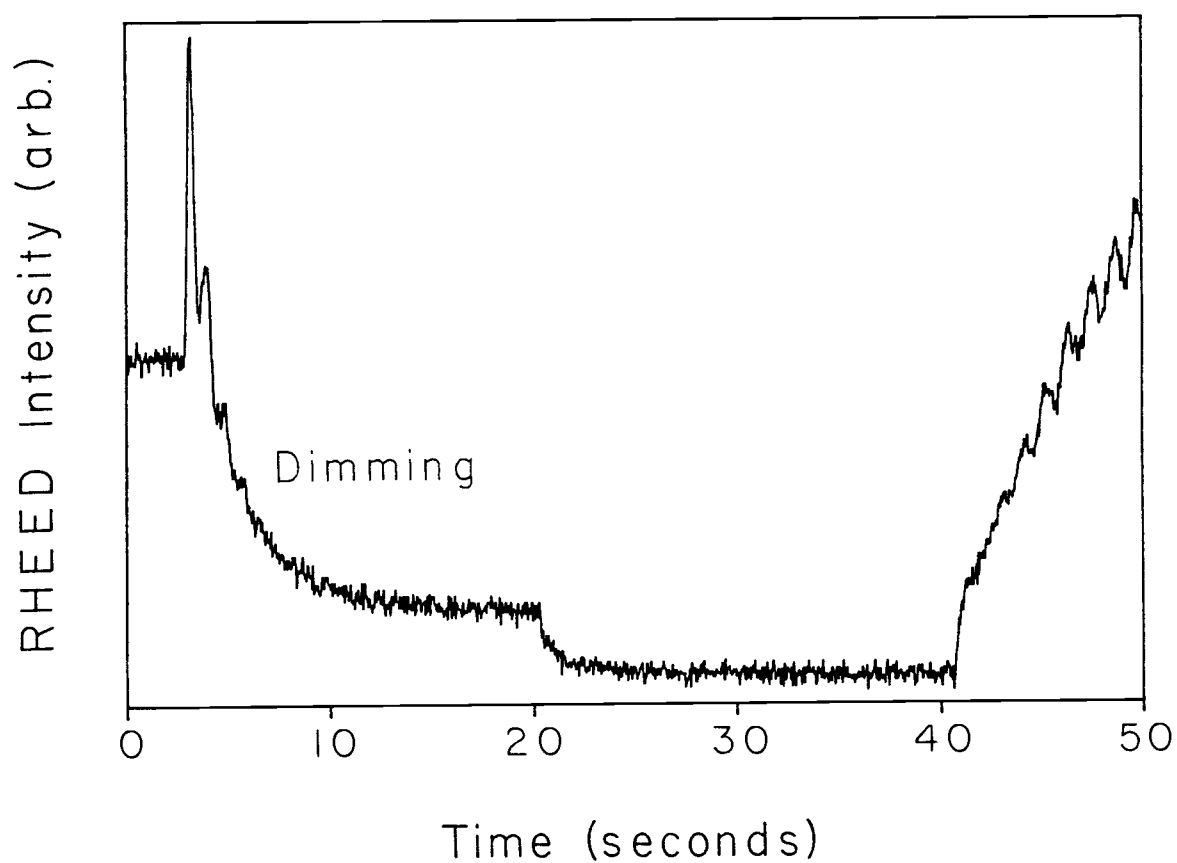


Figure 10
RHEED oscillations of strained InGaAs growth on GaAs. The intensity of the RHEED pattern dims as InGaAs is grown which shows up in the oscillations as the decay in intensity over time.

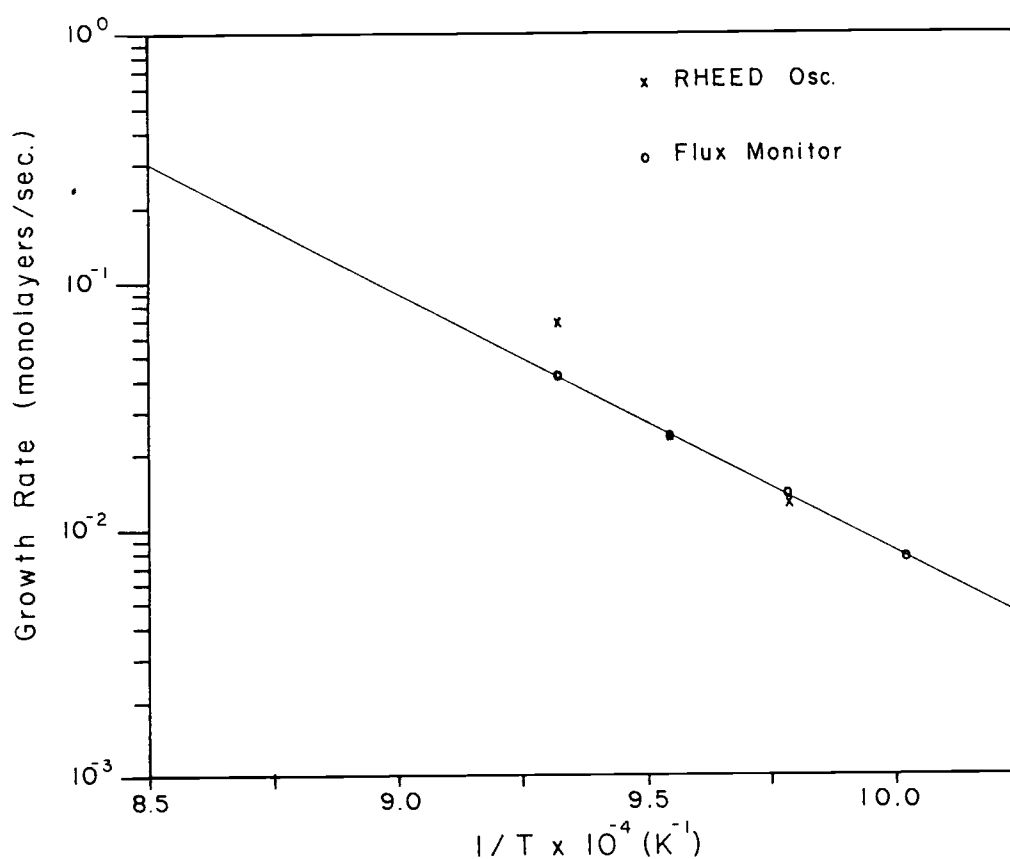


Figure 11

Indium oven flux as a function of oven temperature as measured by RHEED oscillations and flux monitor. The indium oven temperature which yields the lattice matched composition, $\text{In}_{.47}\text{Ga}_{.53}\text{As}$, can be found by extrapolation of this line to higher temperatures. An approximate indium oven temperature of 873°C results from this extrapolation.

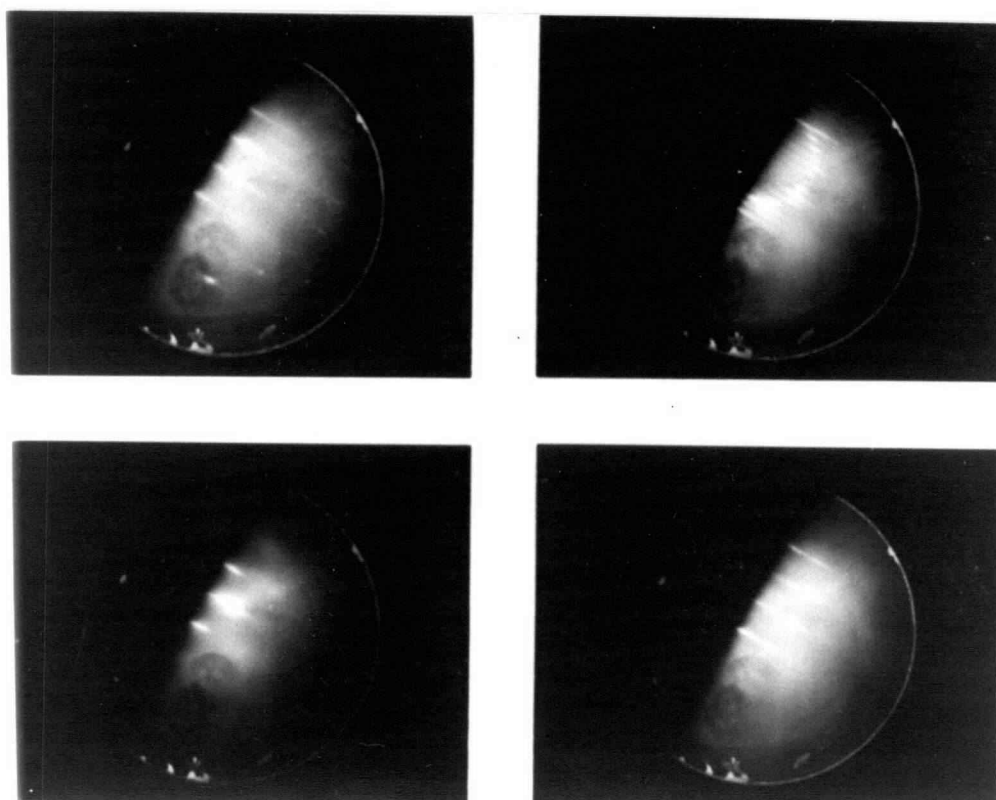


Figure 12

Photographs of RHEED patterns of arsenic and gallium stabilized surface reconstructions of InGaAs grown on InP. The upper photographs show the arsenic stabilized reconstruction in the two $\langle 110 \rangle$ directions. The lower photographs show the gallium stabilized reconstruction in the same $\langle 110 \rangle$ directions.

metal shutters are closed. This metastability in the surface reconstructions is only observed at arsenic fluxes which are low, i.e., close to the transition to metal stabilized, and when the substrate temperature is below 500° C.

RHEED oscillation measurements have been made for unstrained, compressively strained, and tensionally strained InGaAs growth on InP. These are shown in Figure 13. The measurements were made in the $\langle 100 \rangle$ direction on the specularly reflected beam. The sample angle with respect to the electron gun was set to give the maximum oscillation intensity.

The films which were grown at the lattice matched composition showed a slightly hazy surface. An SEM picture of a typical surface is shown in Figure 14. These defects are thought to arise from polishing damage in the substrate which propagated into the film. The majority of the substrates used were polished by hand. Other sources of these defects could be lattice strain, and contaminants on the initial surface. On some substrates trace amounts of sulphur were observed in the initial Auger spectra and in a number of the films oxygen was also found in the final Auger spectra. This indicates a leak in the system at the time of growth. Both of these contaminants could cause defect formation in the film.

PL spectra from these lattice matched films displayed a bright peak at 1.588 micron wavelength at 77° K. The PL spectra is shown in Figure 15. Without knowing what the residual impurities present in the film are, the exact composition cannot be extracted from these measurements. The luminescent efficiency is high, comparable to $\text{In}_{.47}\text{Ga}_{.53}\text{As}$ grown by Liquid Phase Epitaxy (LPE). This high efficiency

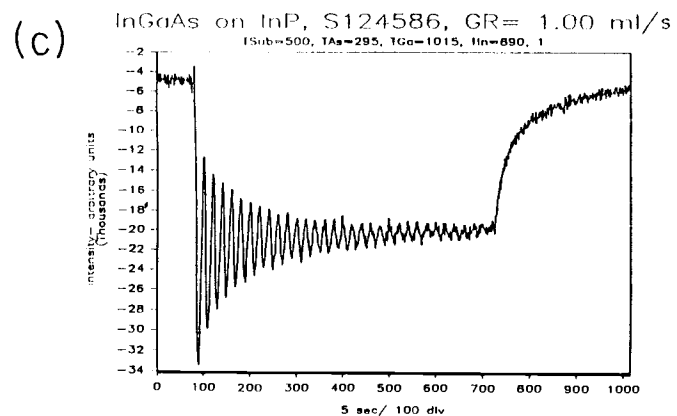
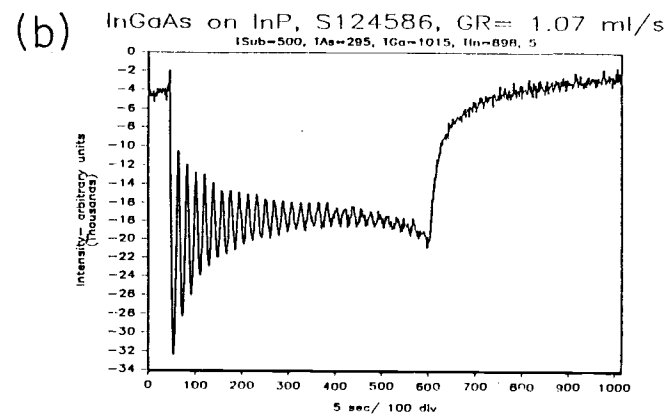
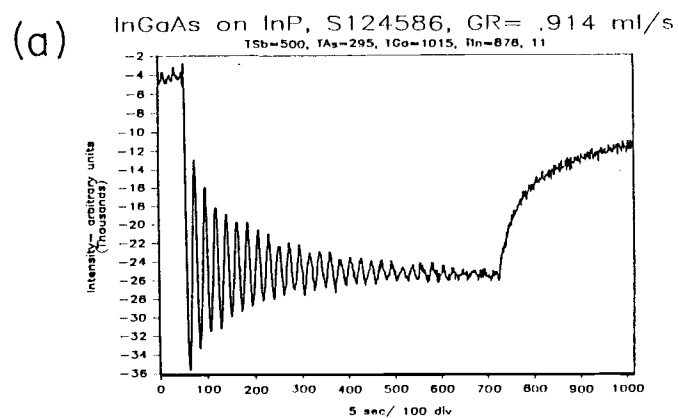


Figure 13
 RHEED oscillations of tensionally strained (a), and compressively strained (b), and unstrained (c) InGaAs grown on InP. The intensity of the RHEED pattern does not dim when InGaAs is grown strained on InP as it does when it is grown strained on GaAs.

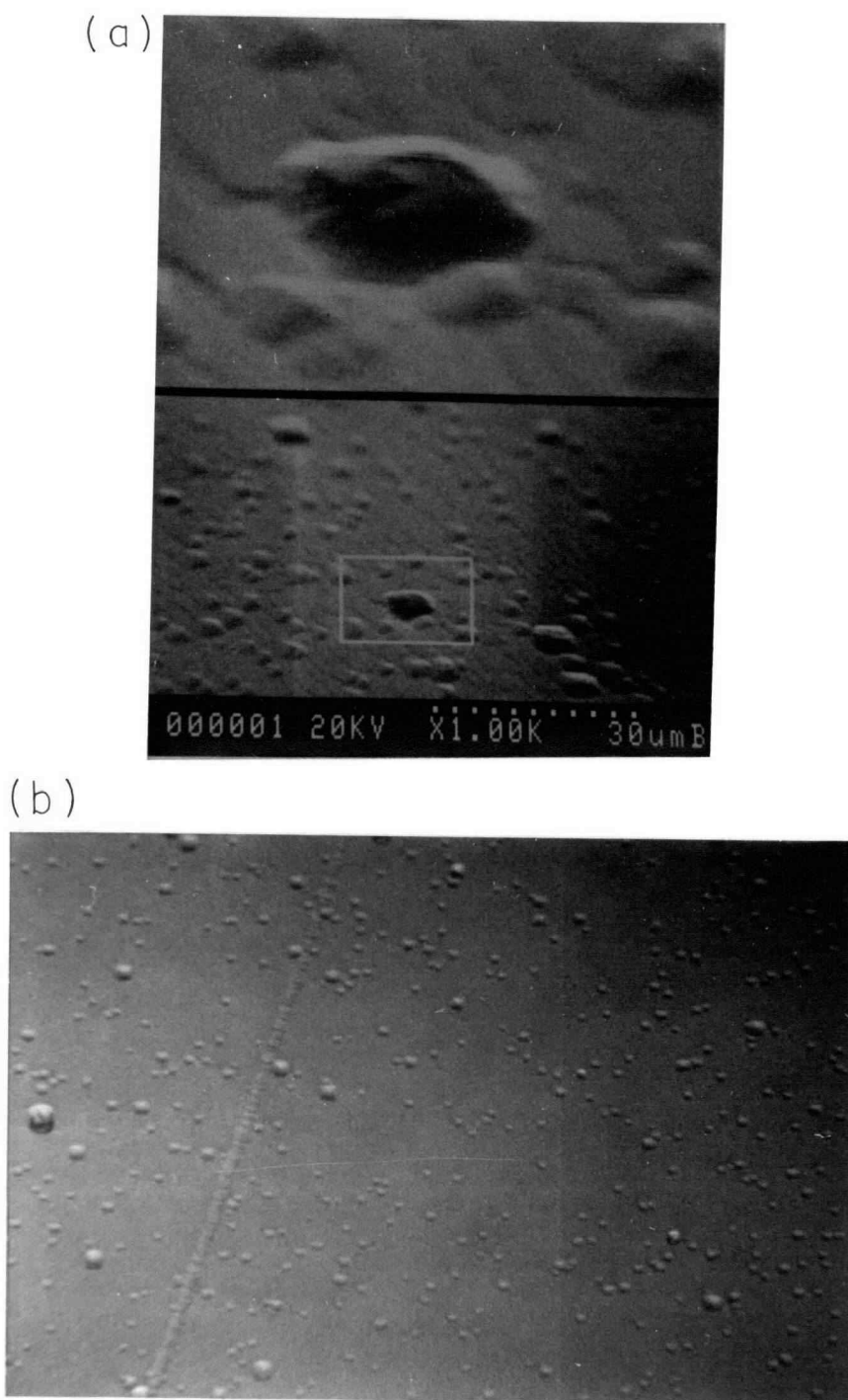


Figure 14

SEM micrograph of surface defects on 1 micron thick lattice matched InGaAs grown on InP (a), normarski interference optical micrograph, 400x, of the same surface (b). The origin of the defects is uncertain, but they are possibly due to polishing defects in the initial surface.

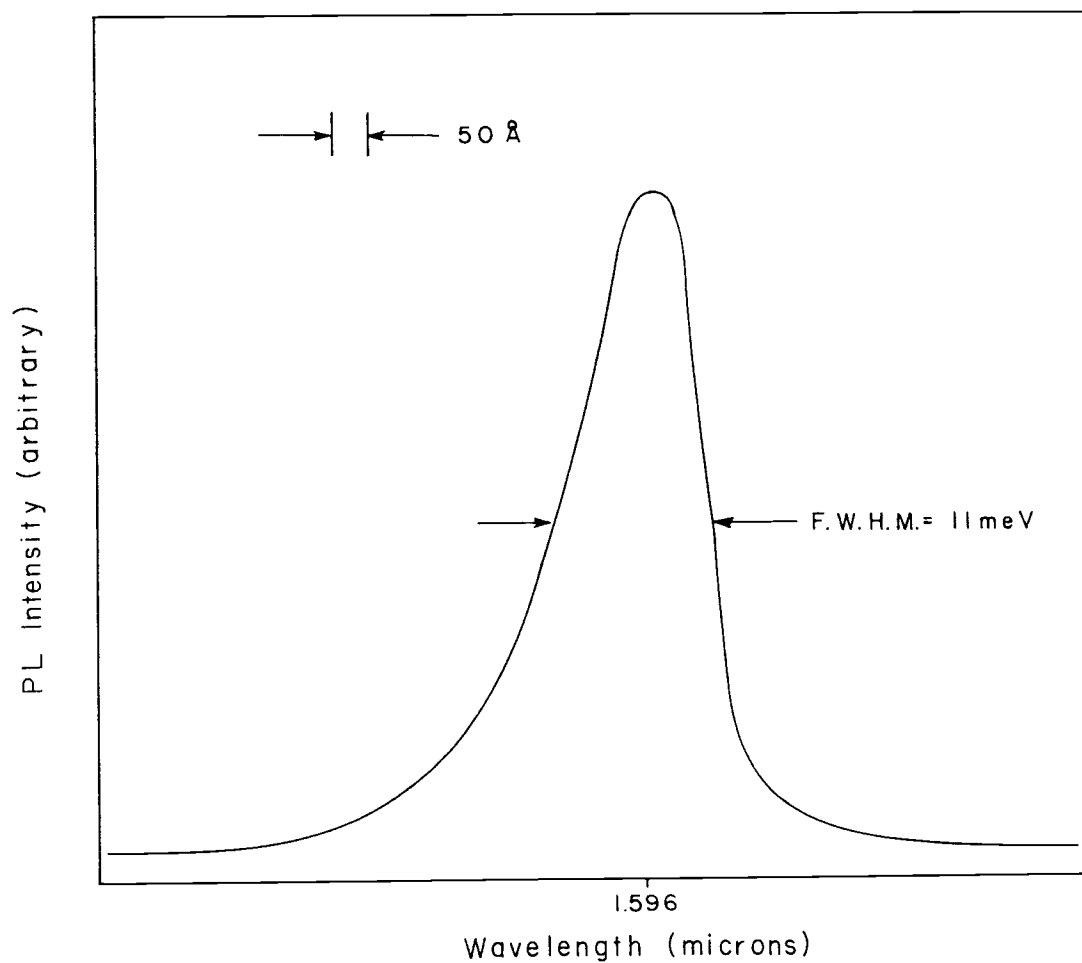


Figure 15
PL spectra from a 1 micron film of InGaAs film lattice matched to InP.
The energy of this transition is .78 eV, and the width is 21 meV.

implies that the composition is close to lattice matched, i.e., radiative transitions dominate the recombination process. This would not be true if the film was far from lattice matched. Misfit dislocations and other defects would decrease the non-radiative recombination lifetime, and with it the luminescent efficiency.

The growth of InGaAs on GaAs also yielded interesting results. Auger sputter profiles from the 75 angstrom thick $\text{In}_{.20}\text{Ga}_{.80}\text{As}$ layers, capped with 75 angstroms of GaAs, are shown in Figure 16. The layers were grown at different substrate temperatures between 495° C and 590° C. The indium concentration is plotted as a function of sputter time, which is proportional to depth in the film, the surface is at $t = 0$ minutes.

Samples similar to those sputter profiled, except having a 1200 angstrom capping layer, were grown and PL spectra were measured. These spectra are shown in Figure 17. The transition energies associated with these quantum wells increases as the substrate temperature during growth is increased. The intensity of these transitions is extremely high, these are the brightest materials measured in the PL laboratory at OSU to date. The linewidth of these transitions is typically a few meV at 13° K.

A different series of samples, each of which containing 4 quantum wells were grown and SIMS, TEM, and PL were done for comparison. These samples each contained quantum wells of 25, 50, 100, and 200 angstroms width, and were grown at a substrate temperature of 530° C. The compositions were $\text{In}_{.05}\text{Ga}_{.95}\text{As}$, and $\text{In}_{.10}\text{Ga}_{.90}\text{As}$. The SIMS spectra obtained from these samples are shown in Figure 18. A high surface concentration of indium is evident in both spectra supporting the other

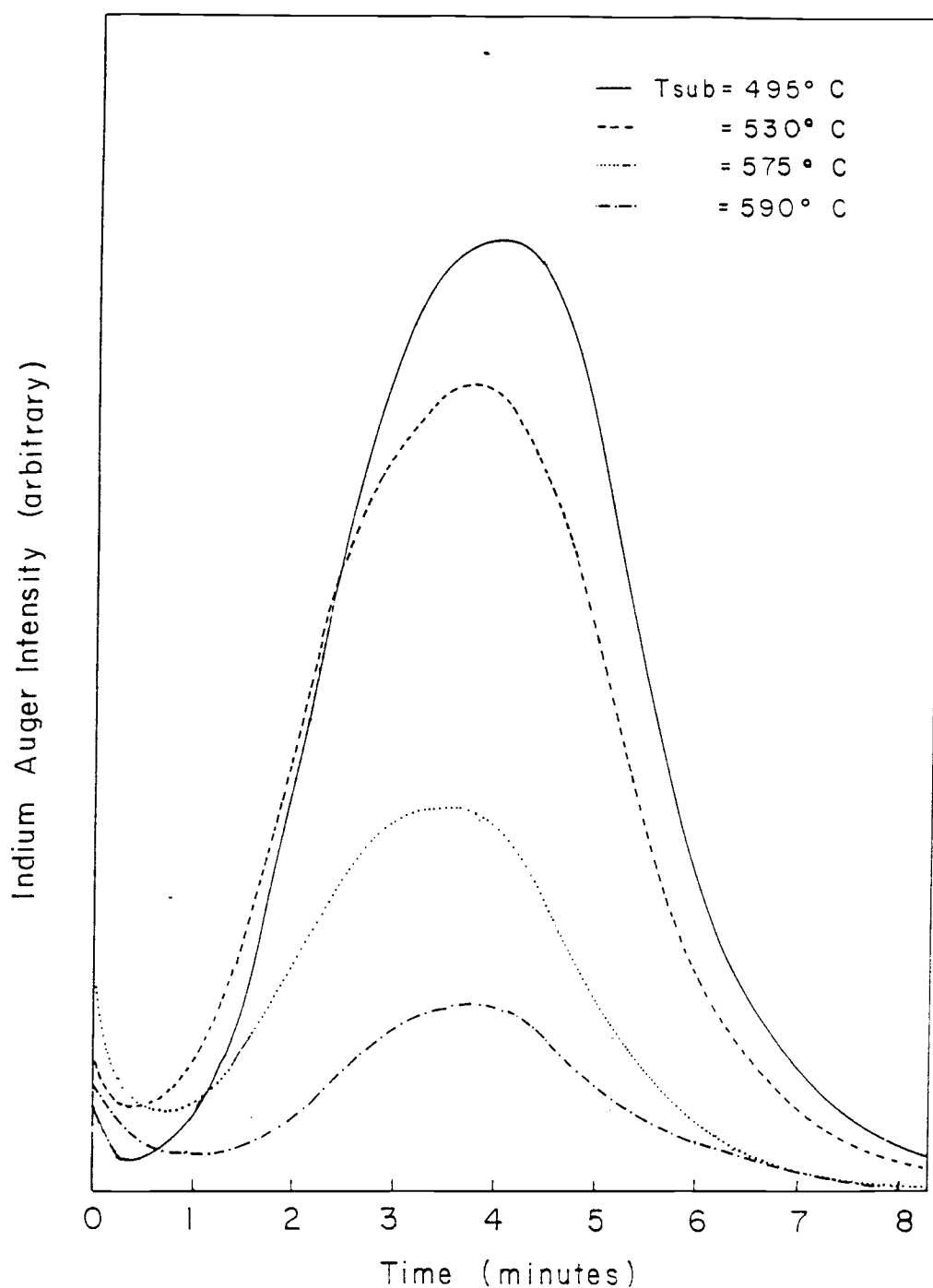


Figure 16

Auger profiles of InGaAs grown on GaAs at various substrate temperatures between 495°C and 590°C . The higher substrate temperatures increased the indium re-evaporation from the growing surface.

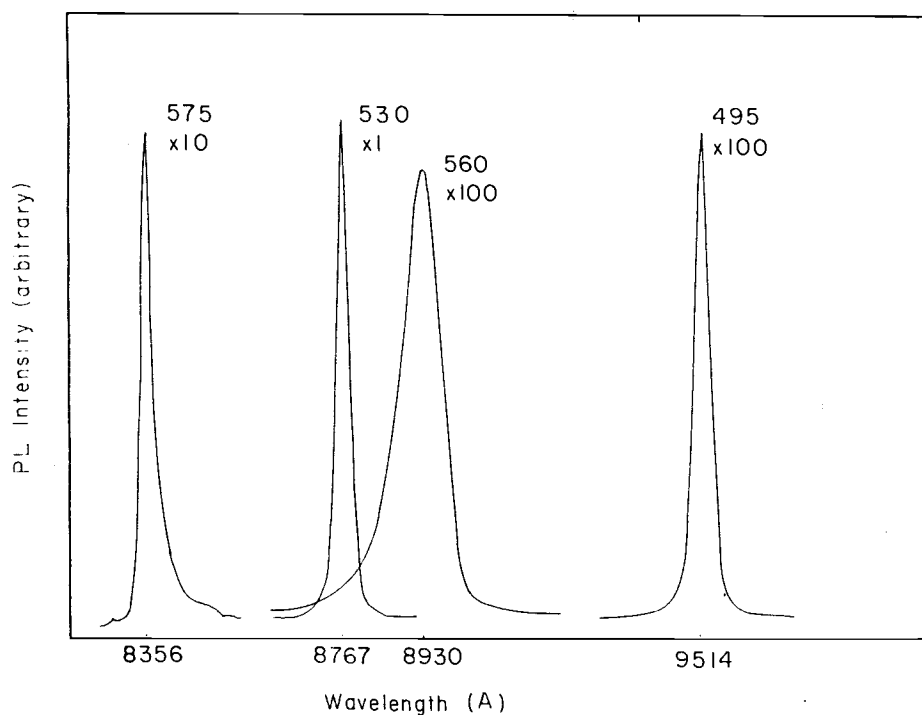


Figure 17

PL spectra of 75 angstrom $\text{In}_{0.20}\text{Ga}_{0.80}\text{As}$ quantum wells grown at substrate temperatures between 495°C and 590°C . Increased substrate temperature during growth reduced the indium incorporated and caused the PL transition to shift to shorter wavelength. The anomalous data at a substrate temperature of 560°C is thought to be due to misfit dislocation formation.

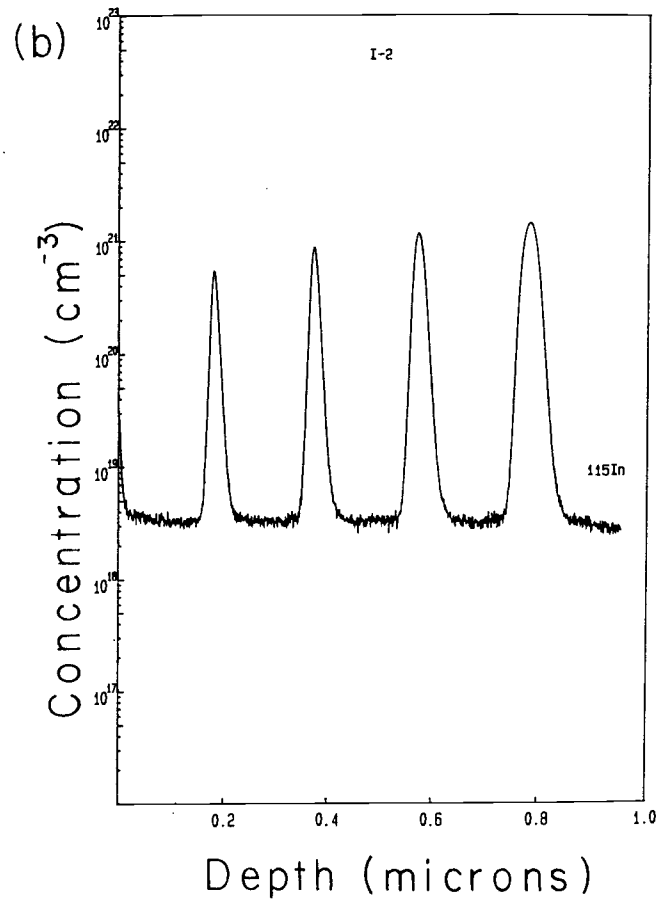
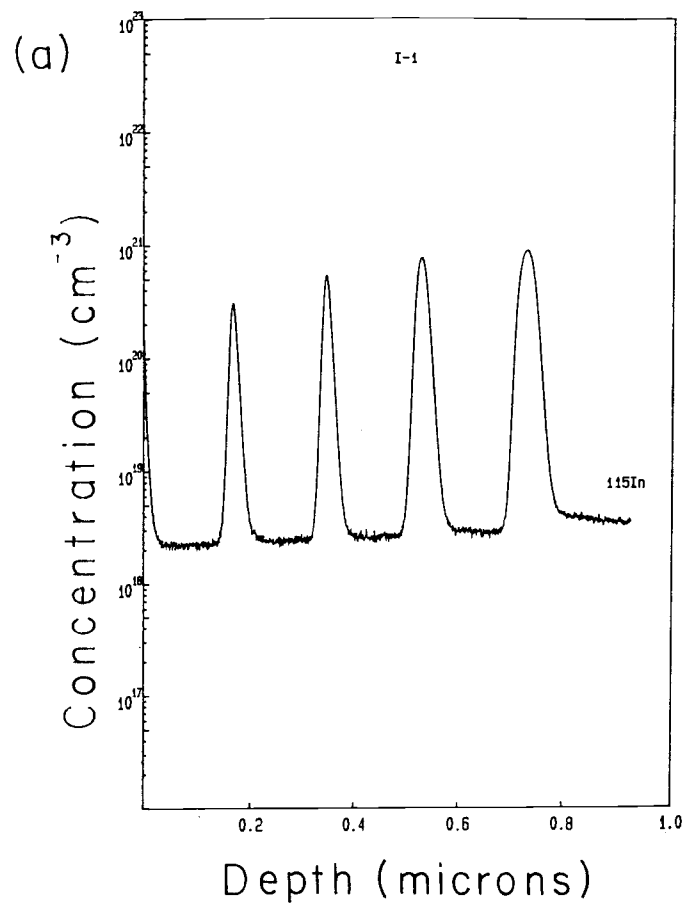


Figure 18
SIMS spectra of multiple quantum wells of $\text{In}_{0.05}\text{Ga}_{0.95}\text{As}$, (a), and $\text{In}_{0.10}\text{Ga}_{0.90}\text{As}$, (b), grown on GaAs. The wells are broadened by the limited depth resolution of SIMS. Indium is clearly resident on the surface.

evidence for surface segregation. The wells appear wide due to the limited depth resolution of SIMS.

TEM micrographs of these structures are shown in Figure 19. These show clearly defined quantum wells of the appropriate thicknesses. This indicates that the indium concentration is not dramatically affected by the segregation or subsequent diffusion. PL spectra from these structures are shown in Figure 20. These show a series of bright peaks, one from each of the wells in each sample. These peaks are similar in intensity and linewidth to the PL spectra of the other InGaAs single quantum well samples grown on GaAs.

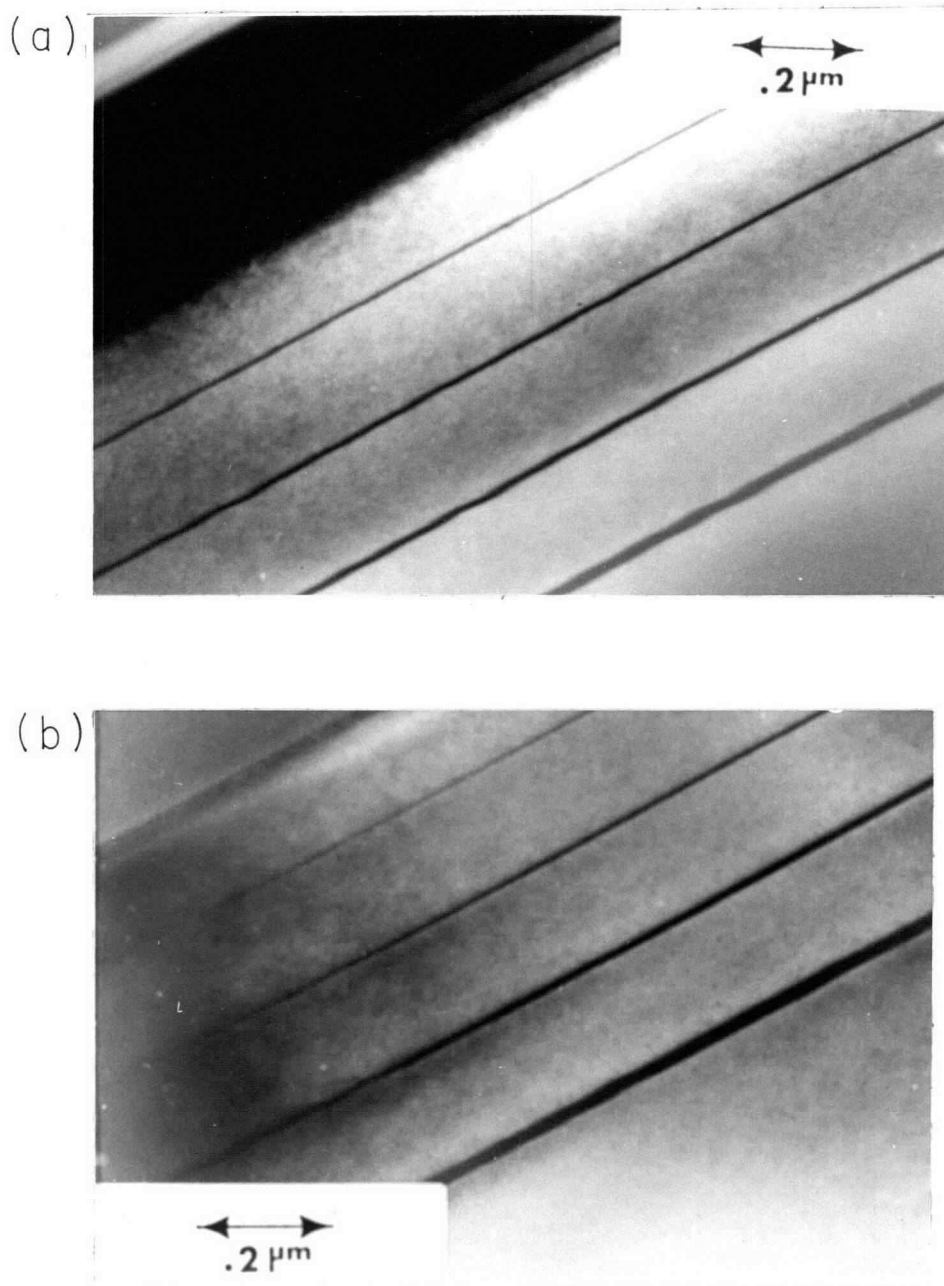


Figure 19
TEM micrographs of quantum wells of $\text{In}_{.05}\text{Ga}_{.95}\text{As}$, (a), and $\text{In}_{.10}\text{Ga}_{.90}\text{As}$, (b), grown on GaAs . The quantum wells are reasonably abrupt and close to the desired width of 25, 50, 100 and 200 angstroms.

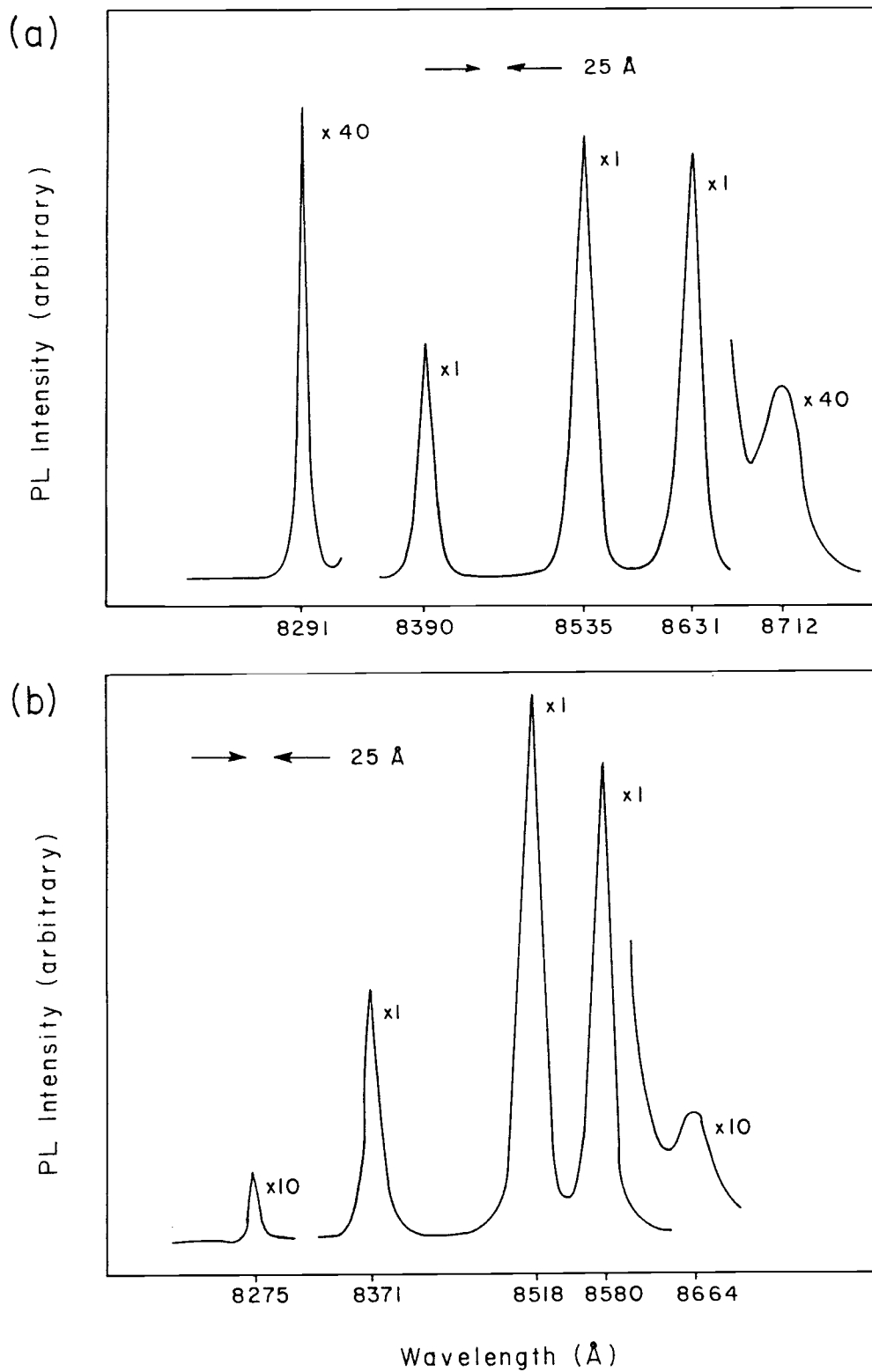


Figure 20
 PL spectra of quantum wells of $\text{In}_{0.05}\text{Ga}_{0.95}\text{As}$, (a), and $\text{In}_{0.10}\text{Ga}_{0.90}\text{As}$ grown on GaAs, (b).

DISCUSSION

The PL results from the $\text{In}_{.47}\text{Ga}_{.53}\text{As}$ growth on InP indicate that the indium and gallium oven temperatures, which yield the lattice matched composition, can be established using RHEED oscillations. This method could also be applied to the growth of $\text{In}_{.48}\text{Al}_{.52}\text{As}$, another ternary which lattice matches to InP. This has not been attempted, but should not be difficult (RHEED oscillations of AlAs have been used to set the aluminum oven temperature to yield a specific aluminum flux in the growth of AlGaAs on GaAs).

The experiments on the growth of InGaAs on GaAs also yielded interesting results. In the Auger sputter profiling of 75 angstrom thick $\text{In}_{.20}\text{Ga}_{.80}\text{As}$ films capped by 75 angstroms of GaAs, shown in Figure 16, the area under each profile is proportional to the amount of indium incorporated into the film. These profiles clearly indicate loss of indium from the film at higher substrate temperatures. The profiles also show an indium concentration which initially decreases as a function of depth, and then increases as the InGaAs layer is approached. This implies that indium segregates to the surface during growth. The SIMS results, Figure 18, corroborated this, also showing a high indium concentration on the surface after the growth of InGaAs quantum wells.

Segregation is believed responsible for dimming of the RHEED diffraction features observed during InGaAs growth. This causes the intensity decay in the RHEED oscillations as seen in Figure 21. The indium surface concentration builds as the InGaAs film grows reducing the diffraction intensity. When growth of the InGaAs layer is terminated, by closing the indium shutter while leaving the gallium

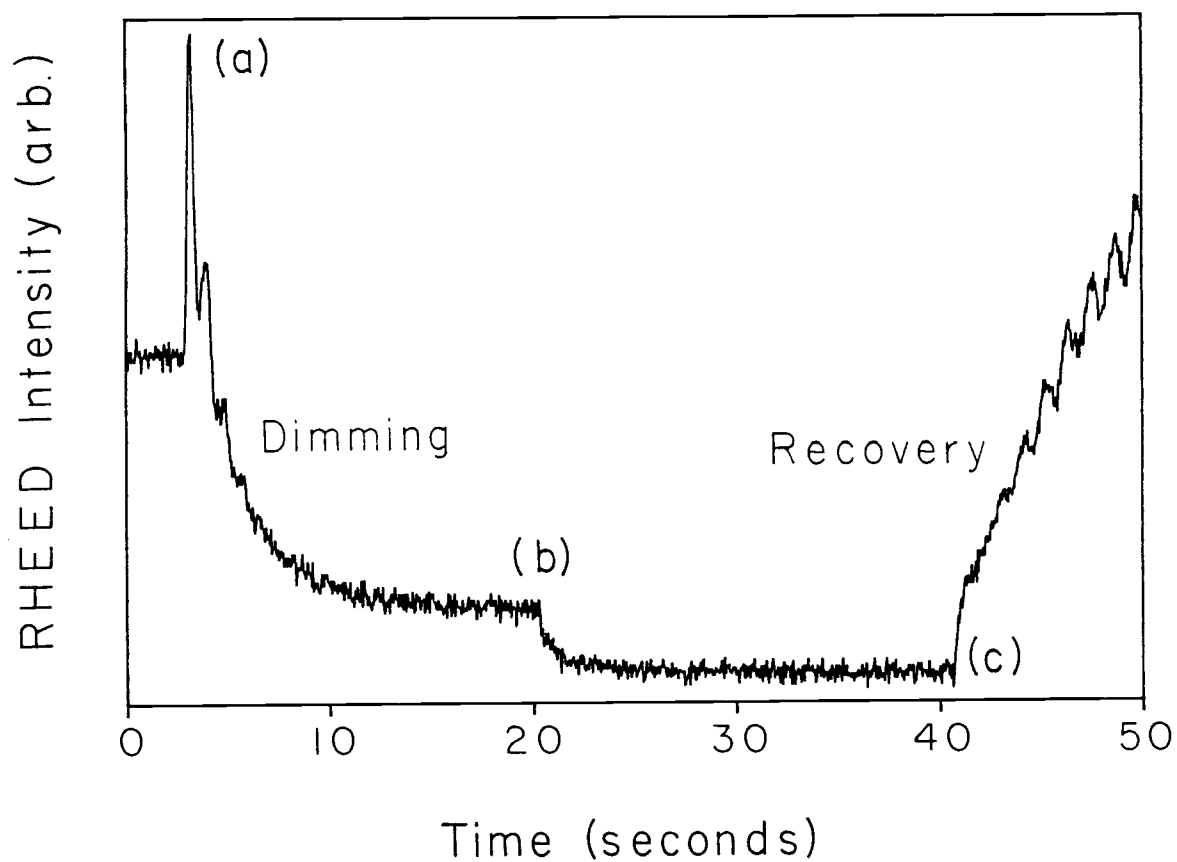
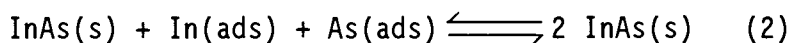
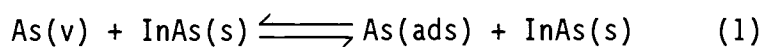


Figure 21

RHEED oscillation measurement of InGaAs growing on GaAs showing the dimming of the RHEED pattern and the recovery. The gallium and indium shutters are opened at (a), they are both closed at (b), and the gallium is re-opened at (c).

shutter open, the indium incorporates into the film and the RHEED pattern slowly recovers to its original brightness. This recovery is also indicated in Figure 21.

While the RHEED pattern is dim there is a high concentration of excess indium adsorbed onto the surface. The loss of indium at increased substrate temperature is through the re-evaporation of this adsorbed indium. Re-evaporation should also be a function of the arsenic flux impinging upon the surface, as shown by the following reactions.



Increase in the arsenic flux will force reaction (1) to the right by mass action. This will in turn force reaction (2) to the right increasing the formation of the compound, and thus the incorporation of indium. These ideas were tested by growing two samples at a substrate temperature of 570° C with different arsenic fluxes. The arsenic oven temperatures used were 385° C and 405° C. The arsenic flux increased three-fold, at 405° C, over what it was at 385° C. The sample was sputter profiled and the results are shown in Figure 22. The increased arsenic flux clearly increased the amount of indium incorporated into the film.

The amount of indium remaining on the surface after growth is determined by the relative rates of two competing processes: segregation and re-evaporation. The effect of this competition can be seen by plotting the ratio of the surface concentrations of indium and

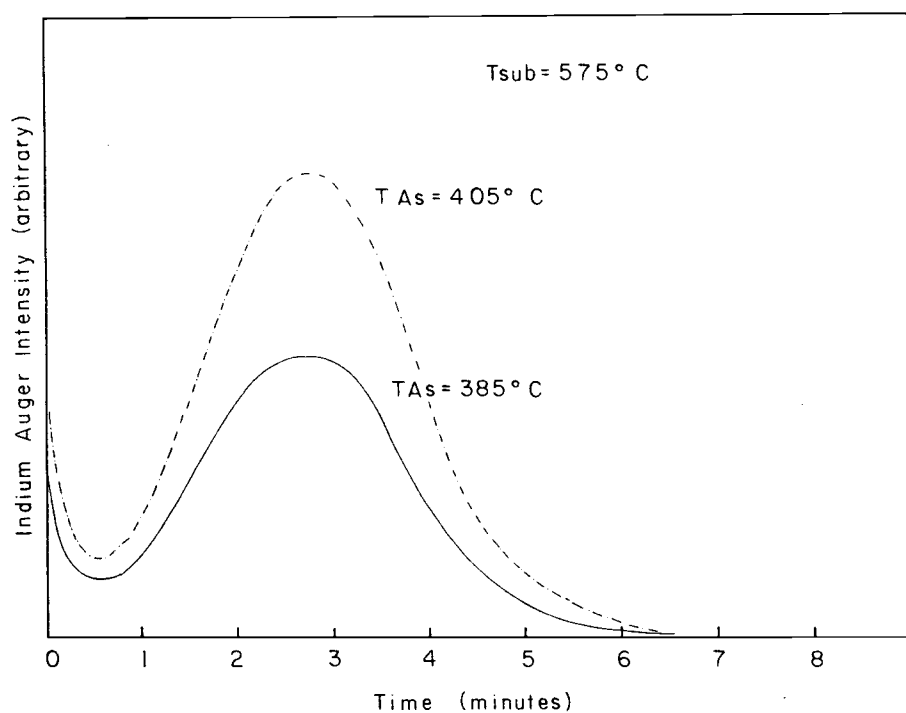


Figure 22
 Auger sputter profile of 75 angstroms of $In_{.20}Ga_{.80}As$, capped by 75 angstroms of GaAs grown at a substrate temperature of $570^{\circ}C$, at two different arsenic fluxes. The increased arsenic flux inhibited indium re-evaporation from the growing film.

gallium against substrate temperature. This is shown in Figure 23. At low substrate temperatures, below 520° C the amount of indium on the surface is small since segregation is reduced at low temperature. At moderate substrate temperatures, 520° C to 560° C, the surface concentration of indium is the highest. The temperature is high enough to allow segregation, but not high enough for appreciable indium to re-evaporate. At high temperatures, above 560° C, segregation occurs, but the surface concentration is diminished by re-evaporation.

The PL results from the quantum well samples with similar structures as those sputter profiled also suggest the loss of indium. This is seen, in Figure 17, by the shift of the PL peak to higher energies at higher substrate temperatures. These transitions are probably due to exciton recombination. This is thought because of their narrow linewidth, and the fact that the peak intensity was measured to change faster than linear with excitation intensity.

The spectrum obtained from the sample grown at a substrate temperature of 560° C is anomalous in both energy and linewidth. The linewidth of the spectrum from this sample is much broader than that of the other quantum wells, and the transition occurred at a lower energy than was expected from the spectra obtained from samples grown at 530° C and 575° C. Similar effects have been observed previously in strained InGaAs, grown on GaAs, by Anderson and co-workers¹⁷, and are thought to be due to misfit formation. The formation of misfits allows the film to relax to its natural lattice constant and unstrained band gap. This would create a shift to lower energy. The change in linewidth was also observed but not explained.

A possible explanation for the remarkably high intensity of the

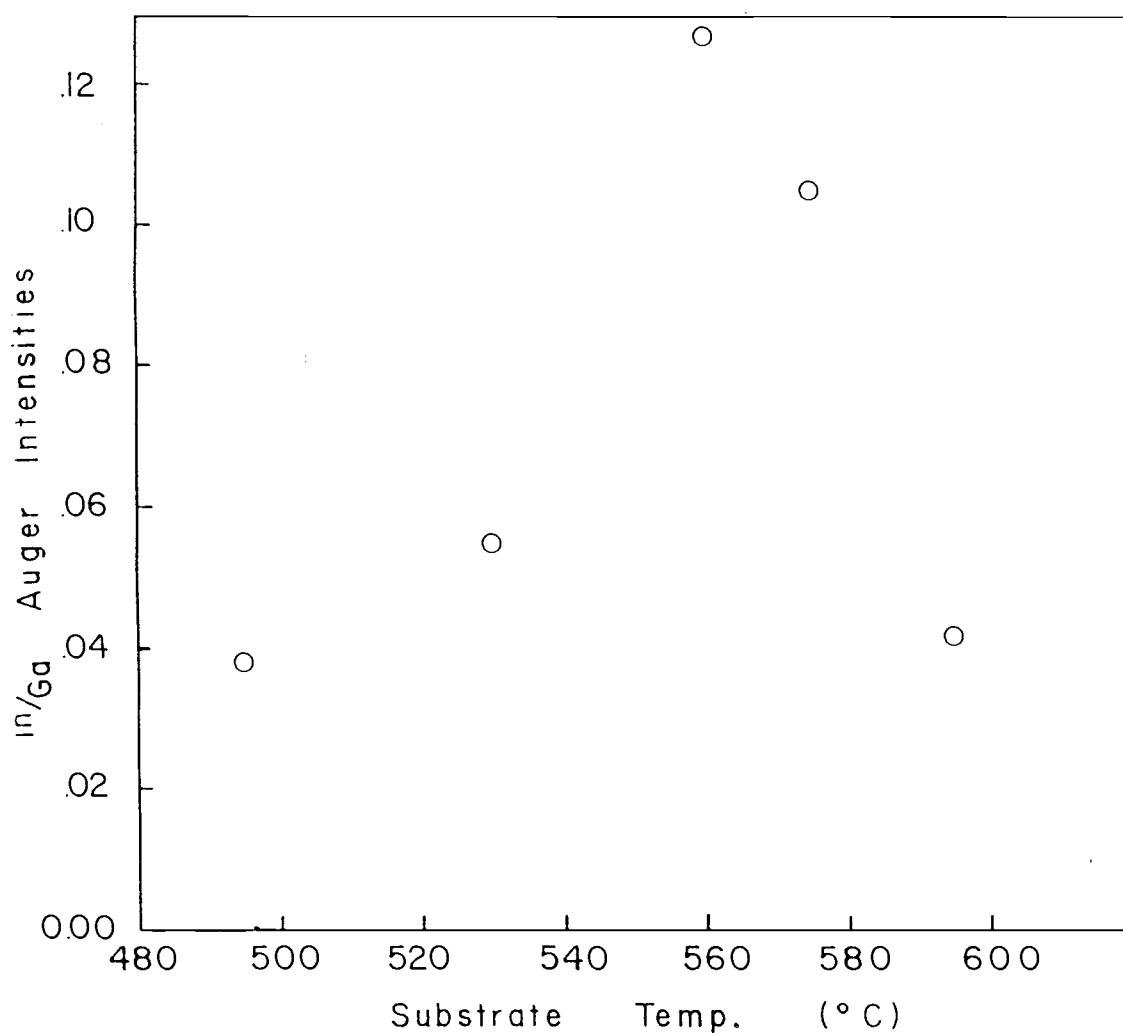


Figure 23

The ratio of the surface concentrations of indium and gallium after growth of 75 angstroms of $\text{In}_{.20}\text{Ga}_{.80}\text{As}$ capped by 75 angstroms of GaAs, as a function of substrate temperature. The maximum segregation was observed at a substrate temperature of 560°C .

PL from these quantum wells involves the indium segregation. The indium which segregated to the surface during the growth of the well both evaporates from the surface and incorporates into the growing film. The incorporation is driven by the concentration gradient between the surface and the bulk. As the surface concentration decreases with time, due to evaporation, the indium incorporated in the film also decreases. This creates a graded InGaAs region on the surface side of the well. A region of graded composition would have a graded band gap which would act as a potential³⁷, moving both electron and holes to the quantum well. This increases the efficiency with which the quantum well collects carriers, and correspondingly the luminescent efficiency. A diagram of this structure is shown in Figure 24. The potential use of this luminescent enhancement in optical devices is yet to be explored.

Interesting differences between RHEED oscillation measurement of compressively strained InGaAs growth on InP and on GaAs can be seen in Figure 25. In the growth of InGaAs on InP the average intensity of the diffraction feature does not decay as growth occurs, as it does in the growth of InGaAs on GaAs. This decay is attributed to the segregation of indium, from the film onto the surface, during growth. A number of hypotheses have been developed as to why this segregation occurs in one case, but not the other. The elastic constant of InGaAs with low indium concentration, such as $\text{In}_{0.05}\text{Ga}_{0.95}\text{As}$ is larger than that of $\text{In}_{0.53}\text{Ga}_{0.47}\text{As}$. This suggests that the force on an individual indium atom in the film will be greater in the case of InGaAs grown on GaAs, for equivalent lattice mismatch. This results in greater potential for segregation in the case of InGaAs growing on GaAs.

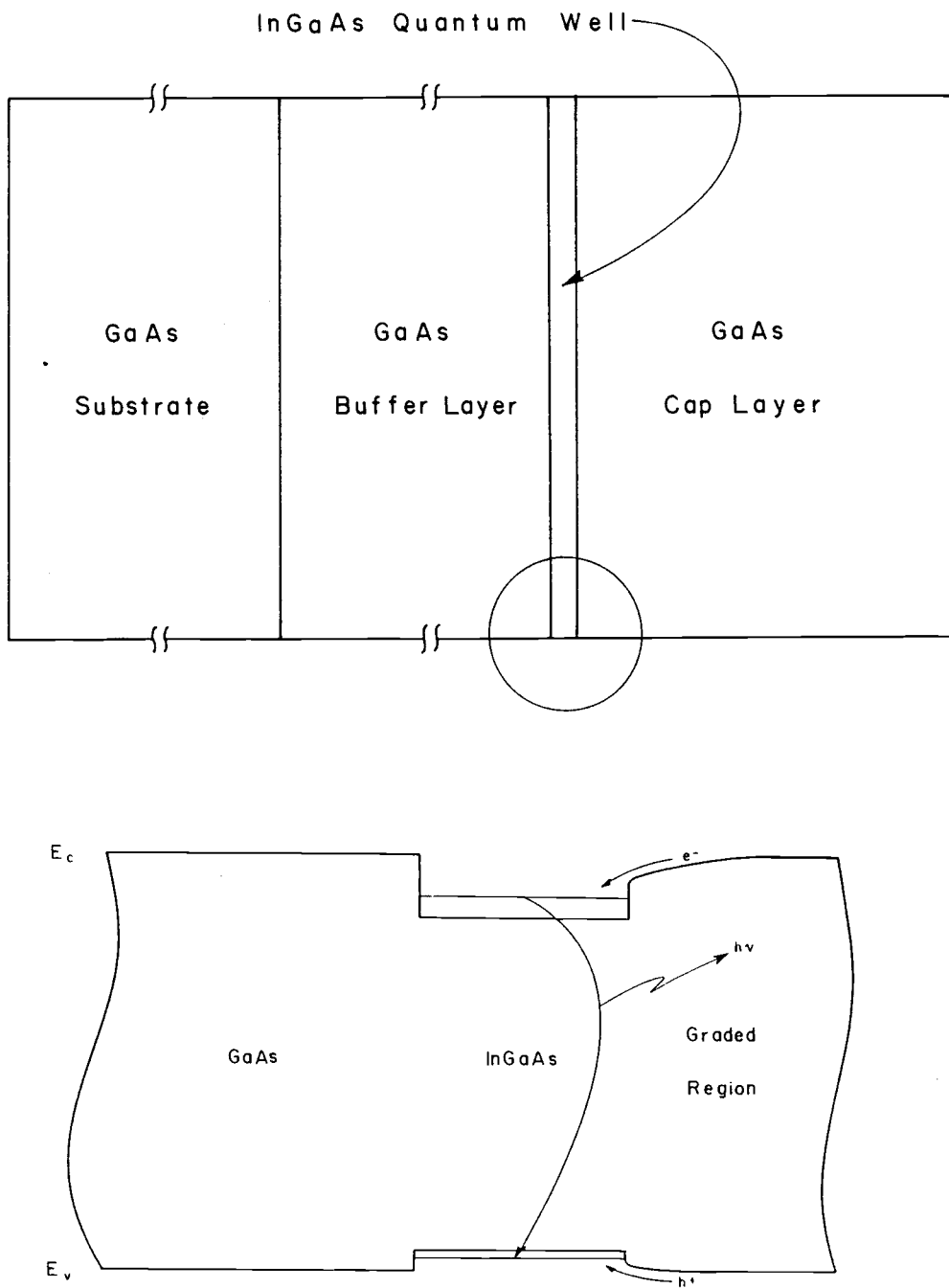


Figure 24

Hypothesized band diagram of InGaAs quantum wells grown on GaAs. The upper diagram shows the structure which was grown. The band diagram of the circled portion is shown in the lower diagram. The graded band gap is due to segregation of indium during growth and would result in intense PL by increasing electron and hole capture from the GaAs cladding layers.

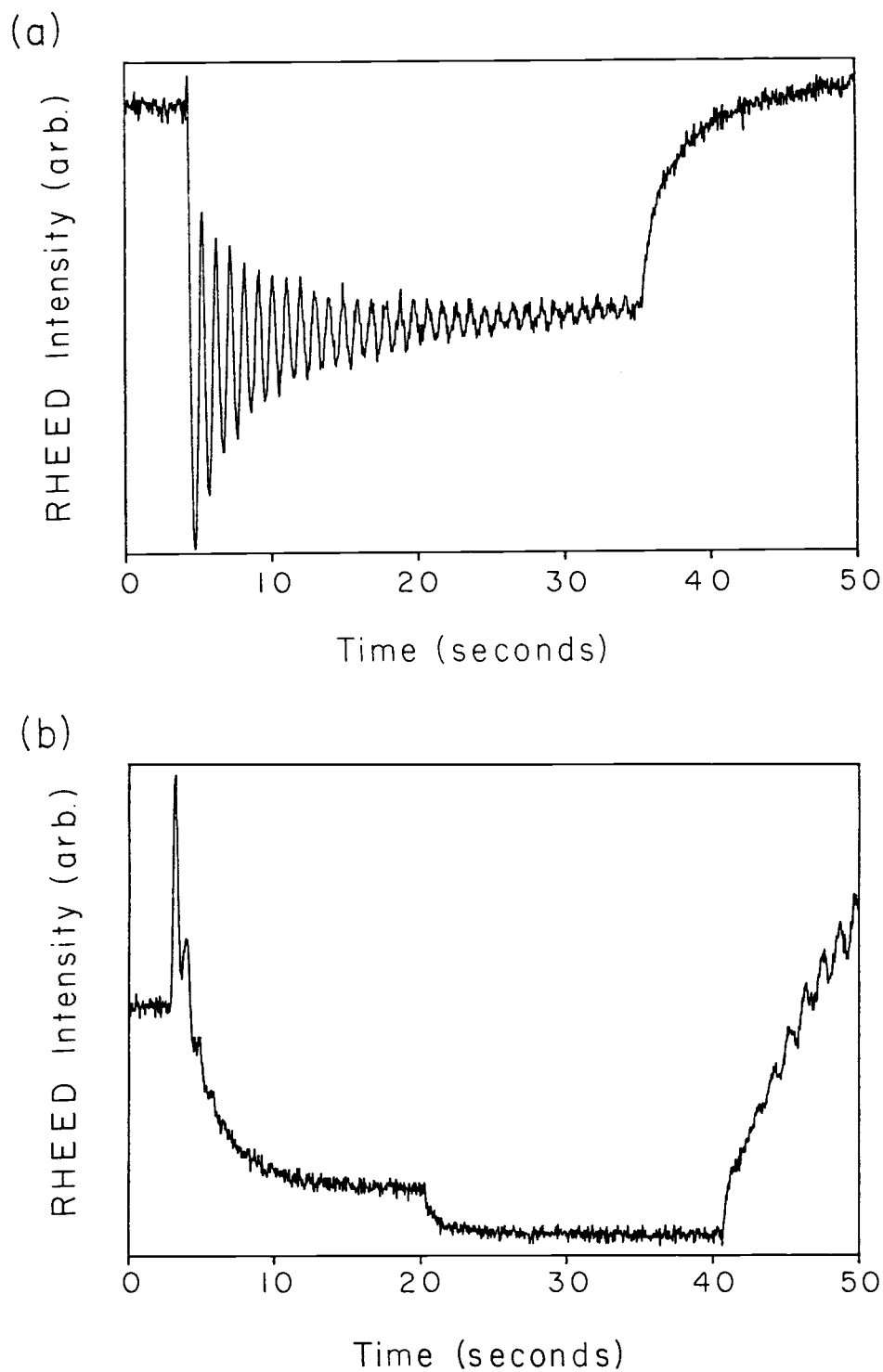


Figure 25
RHEED oscillations from compressively strained InGaAs grown on InP, (a), and on GaAs, (b). Growth upon GaAs shows dimming of the RHEED intensity, while growth upon InP does not.

Another possible explanation involves the localization of the strain around individual indium atoms. In the case of InGaAs growth on GaAs the number of oversized species in the film is fewer, and therefore the strain field around each indium is more localized. In the case of InGaAs growth on InP, the number of indium atoms over which the strain is distributed is greater, and correspondingly the strain field associated with each indium atom is smaller. This also suggests segregation would be more probable in the case of InGaAs on GaAs.

The quantum wells of strained InGaAs grown on GaAs, at a variety of widths, and at .05 and .10 mole fraction indium, showed bright, narrow PL transitions, as seen previously in Figure 15. The expected energies of these transitions can be calculated by solving the quantum mechanical one dimensional finite well problem, if a number of parameters are known. The important parameters are: band gap of the cladding material, band gap of the well material, and how the respective band structures align.

The band gap of GaAs is 1.515 eV at 13° K, while the band gap of InGaAs varies smoothly between that of GaAs and that of InAs according to:

$$E_g = 1.515 - 1.24x + 0.18x^2$$

where x is the mole fraction of indium in the compound¹⁷. As was noted previously biaxial compressive strain widens the band gap, and splits the valence band degeneracy. The light hole band moves to lower energy than the heavy hole band. A first order correction to the band gap, as a function of strain in the film, can be calculated knowing the films

elastic constants, and deformation potential¹⁷. The band gaps of unstrained InGaAs and InGaAs grown strained on GaAs are plotted versus indium mole fraction in Figure 26. The expected values for the quantum well PL transitions calculated using the strain perturbed band gap of InGaAs, and the measured values, are plotted in Figure 27. The calculations fit the data reasonably well for the .10 indium mole fraction quantum wells, but not for the .05 indium mole fraction quantum wells.

The similarity of the PL measurements from these samples implies that there is little difference in composition between the wells. The SIMS measurements on the other hand show more indium in the .10 mole fraction wells, than in the .05 mole fraction wells, as was expected from the RHEED oscillation calibration. These differences may be due to non-uniformity in the indium and gallium ovens across the sample length, and difference in the growth conditions between the two samples. The substrate temperature, and arsenic flux have already been shown to have a strong effect on the amount of indium incorporated, and the beam non-uniformity can be significant. The side of the sample close to the indium oven will have a higher indium mole fraction than the side closer to the gallium oven. The orientation of the sample with respect to the ovens is lost in removing it from the system, and it is not known which side was used for SIMS and which for PL. This problem is usually solved by rotating the sample during growth, but this was not done in these growths so that the RHEED pattern could be observed.

Improving our understanding of the interactions which occur on a growing, strained, surface involves enlarging the number of the

InGaAs bandgap versus In mole-fraction

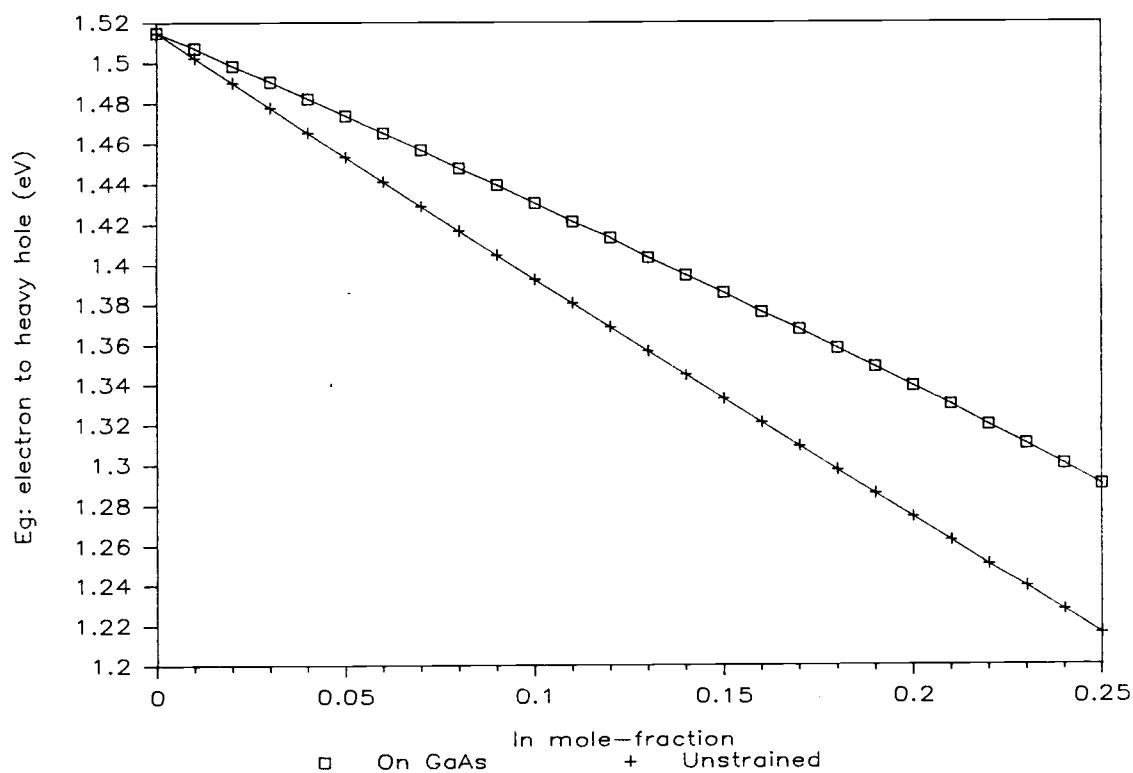


Figure 26

The band gap of unstrained InGaAs, and InGaAs grown on GaAs, as a function of indium mole fraction. Growth of InGaAs on GaAs causes the band gap to widen from what it would be if grown unstrained.

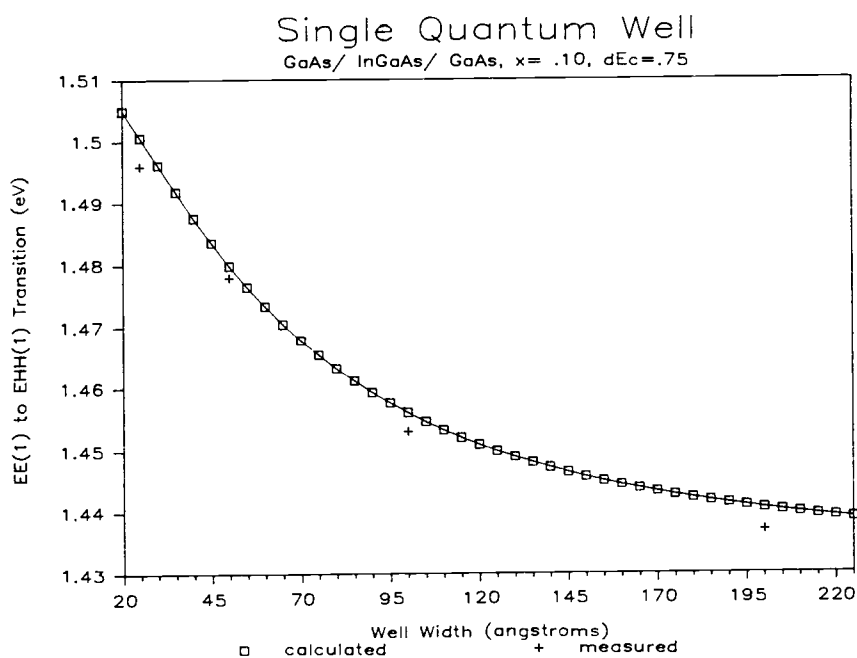
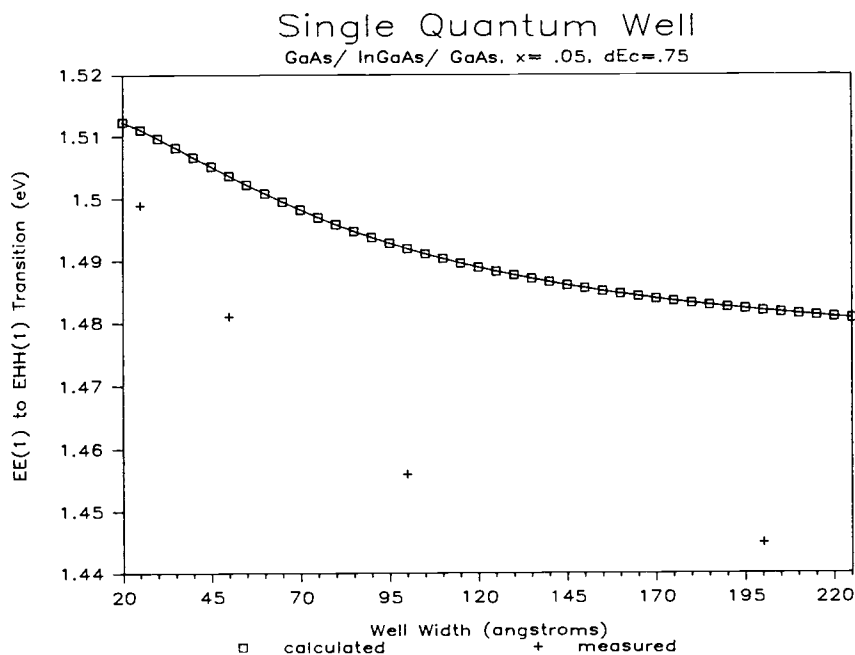


Figure 27

Calculated and measured quantum well transitions for $\text{In}_{.05}\text{Ga}_{.95}\text{As}$ and $\text{In}_{.10}\text{Ga}_{.90}\text{As}$ single quantum wells. The $\text{In}_{.10}\text{Ga}_{.90}\text{As}$ quantum wells fall close to the calculated, but the $\text{In}_{.05}\text{Ga}_{.95}\text{As}$ do not. This is probably due to flux non-uniformity over the sample.

interactions which are considered important. In most of the modeling of MBE growth to date only the reaction of the Group IIIa and Group Va elements is considered, while a large number of other reactions could be very important, e.g., defect incorporation, exchange reactions³⁸, segregation²¹, clustering. A number of these interactions are diagrammed in Figure 28. Detailed knowledge of the importance of each of these interactions is far from complete, but necessary to grow these materials reproducibly.

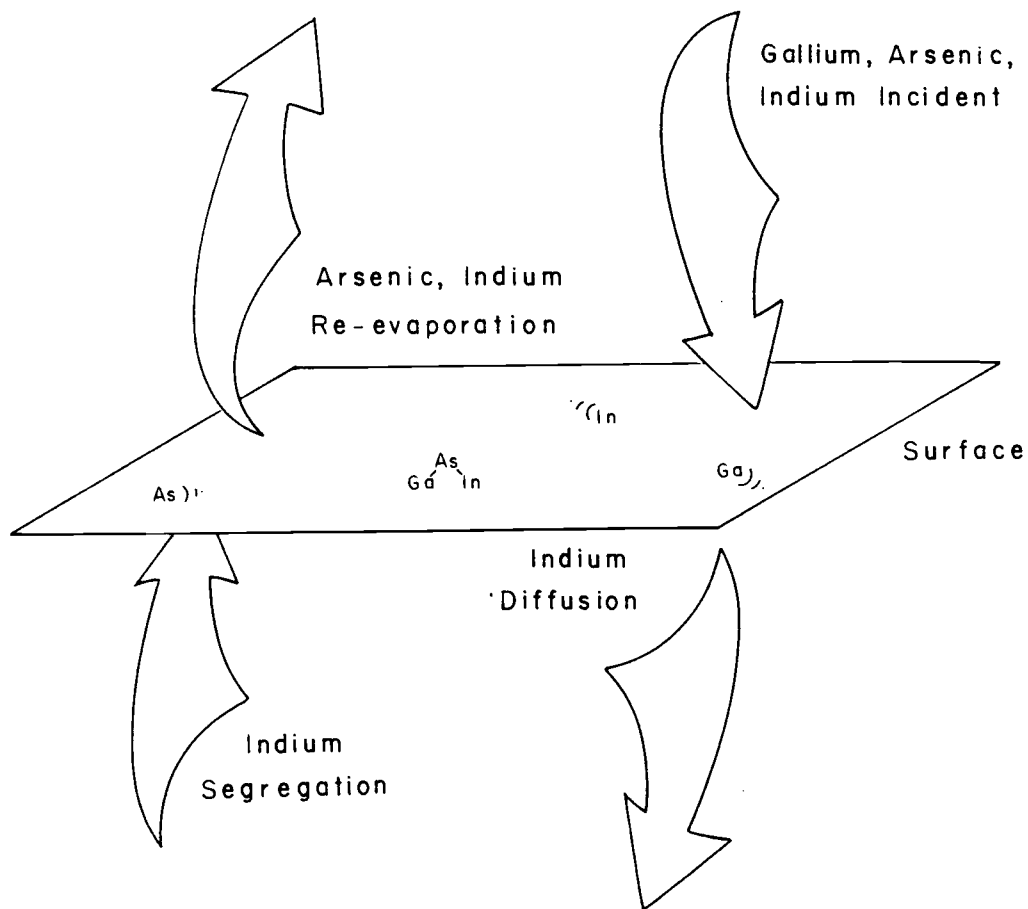


Figure 28

A schematic of some of the important interactions which occur on a growing strained film. These need to include interaction between the film and the bulk, such as segregation and diffusion, as well as the fundamental growth reaction. Other important reactions not shown include the incorporation of defects and exchange reactions.

SUMMARY AND CONCLUSIONS

MBE growth of the III,III-V ternary compound InGaAs has been studied. An in situ calibration method, using RHEED oscillation measurement, has been developed to find accurately the indium and gallium oven temperatures which yield lattice matched film growth on InP substrates. The effect of compressive strain on growth was studied by growing thin films of InGaAs, at low indium mole fraction, on GaAs substrates.

The procedure to find a film with composition lattice matched to InP was tested by growing films and measuring their optical properties via PL spectroscopy. The growth of thin lattice mismatched InGaAs layers on InP has also been shown to be possible without affecting the surface morphology.

Strained InGaAs films grown on GaAs were analyzed via Auger sputter profiling, SIMS, TEM, and PL spectroscopy. It was found that the lattice mismatch induced strain caused the segregation of indium to the surface during growth. This segregation is thought to be responsible for enhancement of photoluminescent intensity of quantum wells. Substrate temperature and arsenic flux have been shown to have a strong affect on the incorporation and segregation of indium during strained InGaAs growth.

Strain can be used to tune a materials properties to a specific device application, e.g., construction of a LASER at 1.3 microns for optical communications. The perturbation which strain imposes on band structure is significant and could be used in the design of novel device structures. The necessity of limiting film thickness, (to avoid misfit dislocation formation), implies that these materials will be

used in quantum wells and strained layer superlattices. Prediction of the resultant properties of these structures involves approximating the perturbation the strain imposes upon the band structure of the individual layers and then calculating the new band gap from quantum mechanical models. The accuracy of these simple approximations is questionable and further experimental verification needs to be done.

The ability to grow strained films with high luminescent efficiency has been demonstrated, but their usefulness in device applications has not yet been established. Operating conditions of optical devices are often stressful, i.e., high electric fields in avalanche photo-diodes, high current densities in LASERs. Issues involving the affect of strain on robustness and reliability, under real operating conditions, are also in need of investigation.

The composition profile of a strained film has been shown to be affected by the interactions occuring on the surface at the time of growth. Better understanding of the processes involved, e. g., segregation and diffusion, is crucial to being able to exploit fully the potential of these materials.

REFERENCES

- ¹ H. C. Casey, Jr. and M. B. Panish, Heterostructure LASERs part B Materials and Operating Characteristics, (Academic Press, San Francisco, 1978).
- ² W. Tsang, Semiconductors and Semimetals vol. 22 part A Materials Growth Techniques, (Academic Press, San Francisco, 1985).
- ³ M. Neuberger, Handbook of Electronic Materials, vol 2, III-V Semiconducting Compounds, (IFI/ Plenum, New York, 1971).
- ⁴ J. H. van der Merve, J. Appl. Phys. **34**, 117 (1963).
- ⁵ J. E. Greene, S. A. Barnett, A. Rockett, and G. Bajor, Applications of Surface Science **22/23**, 520 (1985).
- ⁶ J. J. Harris, B. A. Joyce, and P. J. Dobson, Surface Sci. **102**, L90 (1981).
- ⁷ J. H. Neave, P. J. Dobson, B. A. Joyce, and Jing Zhang, Appl. Phys. Lett. **47**, 100 (1985).
- ⁸ J. M. Van Hove and P. I. Cohen, Appl. Phys. Lett **47**, 726 (1985)
- ⁹ J. Singh and K. K. Bajaj, J. Vac. Sci. Technol. B **2**, 576 (1984).
- ¹⁰ J. R. Arthur, Surf. Sci. **43**, 1999 (1974).
- ¹¹ J Singh and K. K. Bajaj, J. Vac. Sci. Technol. B **3**, 520 (1985).
- ¹² J. Singh, S. Dudley, and K. K. Bajaj, J. Vac. Sci. Technol. B **4**, 878 (1986).
- ¹³ J. Singh, K. K. Bajaj, Appl. Phys. Lett. **47**, 594 (1985).
- ¹⁴ J. W. Matthews and A. E. Blakeslee, J. Cryst. Growth **27**, 273 (1975).

- ¹⁵ J. W. Matthews and A. E. Blakeslee, *J. Cryst. Growth* **27**, 188 (1974).
- ¹⁶ R. People and J. C. Bean, *Appl. Phys. Lett.* **47**, 322 (1985).
- ¹⁷ N. G. Anderson, W. D. Laidig, G. Lee, Y. Lo, and M. Ozturk, *Materials Research Society Proccdings* **37**, 223 (1985).
- ¹⁸ A. Zur and T. C. McGill, *J. Vac. Sci. Technol. B* **3**, 1055 (1985).
- ¹⁹ G. B. Stringfellow, *J. Cryst. Growth* **58**, 194 (1982).
- ²⁰ C. E. C. Wood and B. A. Joyce, *J. Appl. Phys.* **49**, 4854 (1978).
- ²¹ A. Rocket, T. J. Drummond, J. E. Greene, and H. Morkoc, *J. Appl. Phys.* **53**, 7085 (1982).
- ²² F. F. Abraham and C. R. Brundle, *J. Vac. Sci. Technol.* **18**, 506 (1981).
- ²³ W. D. Laidig, P. F. Caldwell, Y. F. Lin, and C. K. Peng, *Appl. Phys. Lett.* **44**, 553 (1984).
- ²⁴ W. T. Tsang, *J. Appl. Phys.* **52**, 3861 (1981).
- ²⁵ K. Mohammed, F. Capasso, J. Allam, A. Y. Cho, and A. L. Hutchinson, *Appl. Phys. Lett.* **47**, 597 (1985).
- ²⁶ A. A. Ketterson, W. T. Masselink, J. S. Gedymin, J. Klem, C. K. Peng, W. F. Kopp, H. Morkoc, K. R. Gleason, *IEEE Transactions on Electron Devices* **33**, 564 (1986).
- ²⁷ K. Y. Cheng, A. Y. Cho, W. R. Wagner, and W. A. Bonner, *J. Appl. Phys.* **52**, 1015 (1981).
- ²⁸ B. I. Miller and J. H. McFee, *J. Electrochem. Soc.: Solid State Science and Technology* **125**, 1310 (1978).
- ²⁹ W. D. Laidig, C. K. Peng, and Y. F. Lin, *J. Vac. Sci Technol. B* **2**, 181 (1984).

- ³⁰ C. Charreaux, G. Guillot, and A. Nouailhat, J. Appl. Phys. **60**, 768 (1986).
- ³¹ N. G. Anderson, W. D. Laidig, and Y. F. Lin, Journal of Electronic Materials **14**, 187 (1985).
- ³² L. Goldstein, M. N. Charasse, A. M. Jean-Louis, G. Leroux, M. Allovon, and J. Y. Marzin, J. Vac. Sci. Technol B **3**, 947 (1985).
- ³³ W. T. Tsang and E. F. Schubert, Appl. Phys. Lett **49**, 220 (1986).
- ³⁴ J. Y. Marzin and E. V. K. Rao, Appl, Phys. Lett. **43**, 560 (1983).
- ³⁵ B. F. Lewis, T. C. Lee, F. J. Grunthaner, A. Madhukar, R. Fernandez, and J. Maserjian, J. Vac. Sci. Technol. B **2**, 419 (1984).
- ³⁶ F. J. Grunthaner, M. Y. Yen, R. Fernandez, T. C. Lee, A. Madhukar and B. F. Lewis, Appl. Phys. Lett. **46**, 983 (1985).
- ³⁷ A. H. Marshak and K. M. van Vliet, Solid- State Electronics **21**, 417 (1978).
- ³⁸ J. A. Van Vechten, J. Cryst. Growth **71**, 326 (1985).
- ³⁹ A. R. Clawson, D. A. Collins, D. I. Elder, and J. J. Monroe, Naval Ocean Systems Center: TN 592, (1978).

APPENDIX

APPENDIX

PROCEDURE FOR POLISHING InP

The goal in polishing is to achieve a smooth, flat, surface free of defects, i.e., scratches, pits. III-V semiconductors are soft materials and therefore difficult to polish, and polish related defects cause structural defects in the epitaxial film which forms above them.

InP (100) wafers ground to a mat finish, are mounted to a glass plate with black wax. They are then hand polished in a solution of 1.5 percent bromine in iso-propyl alcohol. This is done in a fume hood due to the noxious nature of concentrated bromine. The wafers are polished on Pellon cloth, a nylon felt resistant to bromine, which is glued onto a glass plate.

The polishing process involves abraiding the surface with the Pellon cloth at a rate similar to that in which bromine etches the surface³⁹. This minimizes the preferential nature in which the bromine attacks the surface by creating a dynamically changing damage layer for the bromine to attack. Iso-propyl alcohol is used as the carrier solution for two reasons: its viscosity is high so that it acts as a good lubricant, and it undergoes a reaction with bromine to form hydrogen bromide (HBr) and acetone³⁹. This reaction slowly reduces the rate at which the surface is etched. Large amounts of damage are removed quickly at the beginning of the polish when the solution is strong, and as the solution weakens the etch rate slows down so that the proper balance between abrasion and chemical etching is achieved.

The difficulty in this procedure involves knowing when to stop. If polishing is terminated when the bromine solution is too strong an "orange peel" will be seen on the surface. If the polishing is

terminated when the bromine solution is too weak the wafer will look good to the eye but will have a high density of microscopic scratches called "sleeks". You can tell about when to stop polishing by the color of the solution, which fades as the HBr is formed. The optimal time to stop is approximately 25 minutes after mixing a fresh solution. At this point the solution strength and color has been reduced to about half the original.

Immediately after polishing the wafer is sprayed with methanol and rinsed with DI water in an ultrasonic cleaner. The wafer is removed from the wax heating the glass plate on a hot plate and sliding the wafer on to filter paper. The residual wax is dissolved off of the wafer with TCA.

The quality of the resulting surface can be determined by looking at the diffuse scattering of the illumination of a microscope light set to full power. A well polished surface will show no diffuse scattering, and appear dark. A poorly polished surface will appear cloudy and the illuminated spot will be visible on the surface. Normarski techniques can be used to image the damage.